

THE BIOCOMPATIBILITY AND CHARACTERIZATION OF AROMATIC  
THERMOSETTING COPOLYESTER

BY

ESRA ALTUN

THESIS

Submitted in partial fulfillment of the requirements  
For the degree of Master of Science in Mechanical Engineering  
in the Graduate College of the  
University of Illinois at Urbana-Champaign, 2018

Urbana, Illinois

Adviser:

Professor Iwona Jasiuk

## ABSTRACT

The current designs of new biomaterials for bone substitutes or scaffolds focus on achieving biocompatibility and sufficient mechanical properties. In this thesis, we investigated the biocompatibility of synthetic polymers called aromatic thermosetting copolyesters (ATSP) as potential biomaterials for bone replacements (implants). These materials are easy to manufacture and have good mechanical properties such as high tensile strength and high wear resistance. They can be made into bulk, film, foams, and composites. In this thesis, we included all these forms and created a composite by infusing ATSP with 10wt% of hydroxyapatite (minerals of similar compositions as those found in bone). Homogenous distribution of the HA filler improves the physical properties of composite ATSP. In addition to this, having robust adhesive features with metals, high energy absorption limit, and promising tribological properties makes ATSP a strong candidate for different orthopedic implant applications.

This research extended an earlier biocompatibility study of ATSP in which direct contact of fibroblasts cells was used to study neat ATSP and ATSP blends with ultrahigh molecular weight polyethylene (UHMWPE) for total joint arthroplasty. The results demonstrated that cells were able to attach to ATSP, and there was no indication of cell death [1]. Since these previous results looked promising, in this thesis we conducted more extensive studies of the biocompatibility of ATSP.

Chapter 1 describes the biocompatibility investigation of three different compositions (film, bulk, and foam) of neat and composite ATSP by 3-(4,5-dimethylthiazol-2-yl)-2,5-diphenyl tetrazolium bromide (MTT assay) with human osteoblast cell line (hFOB 1.19 (ATCC® CRL 11372™)), and the results were obtained from the metabolic activity of hFOB 1.19 cells for 48 hours. The results which were either equal to or greater than 85% were accepted as non-

cytotoxic, the values between 60% and 85% were defined as slightly cytotoxic, 30%– 59% were moderately cytotoxic, and less than 30% were accepted severely cytotoxic. The results of metabolic activity by MTT showed that each group (film, bulk, and foam) of neat and composite ATSP samples did not demonstrate any toxicity at all concentrations ( $\geq 85\%$ ) except for neat film samples which showed slight toxicity ( $\sim 75\%$ ). Overall, the results for each group were consistent between neat and composite samples. Furthermore, the increase in the concentration did not change the results. The presence of HA was used to investigate the effect of HA on increasing the metabolic cell activity; however, there was no increase in cell activity with the presence of the HA.

Chapter 2 highlights the neat and composite foams that were designed to analyze the effect of biomaterial physical features, including porosity and mineral content over the bone formation by human mesenchymal stem cells differentiation. The analysis was done by alamarBlue® and RT-PCR assays. The metabolic activity results of foam samples by alamarBlue® with MSCs showed that none of the samples demonstrated any toxic effect; the metabolic activity for all samples was higher than initial metabolic activity values. All samples allowed cell proliferation and cell growth. Also, not only mineralized samples but also osteogenic media positively affected the metabolic activity because the composite samples showed higher metabolic activity than neat samples on the day seven. Also, samples in osteogenic media demonstrated the high metabolic activity in comparison with samples in growth media on day seven. RT-PCR results showed that the samples in osteogenic media showed upregulated pattern for all gene expressions. It could also be interpreted that neat and mineralized samples in combination with pure osteogenic media promoted osteogenesis and allowed new bone formation.

## ACKNOWLEDGEMENTS

This study would not have been possible without the help and contributions from many groups and people. I would like to thank Professor Dipanjan Pan and Professor Berendan Harley for sharing his experience with therapeutic materials and giving me the opportunity to use equipment and instruments in their labs to complete the majority of my experiments. I would also like to thank Santosh Misra for the guidance and knowledge he provided throughout the experiments and analysis, and Taylor Kampert and Marley Dewey for teaching me a lot about cell culture methods and cytotoxicity assays. Also, I would thank Jake Meyer for preparing samples. Many thanks to Professor Iwona M. Jasiuk, my adviser, who gave me the opportunity to work in her group, and gave lots of suggestions for my research, and taught me how to become a successful scientist. I could not have accomplished all that I did without all these people's assistance.

Thanks to all members of Jasiuk group for providing assistance that may have been offered throughout my master's studies. I would like to thank staff of Materials Research Laboratory at University of Illinois at Urbana – Champaign for all the trainings and help on all the required instruments in my experiments, and to the Mechanical Engineering Department at the University of Illinois at Urbana-Champaign for the opportunity to conduct research and earn valuable experience in the field of materials science and engineering. Finally, I would like to thank my family and friends for being in my life whenever possible, and supporting me in receiving my Master of Science degree.



*For my family...*

## TABLE OF CONTENTS

<b>LIST OF FIGURES .....</b>	<b>viii</b>
<b>LIST OF TABLES .....</b>	<b>ix</b>
<b>CHAPTER 1: INTRODUCTION .....</b>	<b>1</b>
<b>1.1 Introduction .....</b>	<b>1</b>
<b>1.2 Biomaterials .....</b>	<b>1</b>
1.2.1 Concept of Biomaterials .....	2
1.2.2 Types of Biomaterials .....	4
1.2.2.1 Aromatic Thermosetting Copolyester (ATSP) .....	7
1.2.3 Characterization of Biomaterial.....	9
1.2.4 Mechanical Properties and Performance of Biomaterials .....	10
1.2.4.1 Mechanical performance .....	10
1.2.4.2 Mechanical durability.....	11
1.2.4.3 Physical properties.....	11
1.2.5 History of Biomaterials .....	12
<b>1.3 Biocompatibility .....</b>	<b>12</b>
1.3.1 History of biocompatibility .....	14
1.3.2 Selection of biocompatibility analyses .....	15
<b>1.4 Test Programs and Descriptions.....</b>	<b>19</b>
1.4.1 In-vitro cytotoxicity assays (ISO 10993-5:2009).....	20
1.4.2 Cytotoxicity Evaluation Methods.....	22
1.4.2.1 Cell Morphology.....	22
1.4.2.2 Cell Proliferation .....	23
1.4.2.3 Cell Viability.....	23
1.4.2.4 Enzyme Activity .....	25
<b>1.5 Experiment Setup for ATSP .....</b>	<b>27</b>
<b>1.6 Materials and Methods .....</b>	<b>28</b>
1.6.1 Foam Samples.....	28
1.6.2 Bulk samples .....	29
1.6.3 Film sample.....	30
<b>1.7 Sterilization of Samples .....</b>	<b>32</b>
<b>1.8 Characterization of samples.....</b>	<b>32</b>
1.8.1 Scanning Electron Microscopy.....	32
1.8.2 Micro Computed Tomography .....	34
1.8.2.1 Porosity Calculations of Foam Samples .....	35
<b>1.9 Statistical Analysis .....</b>	<b>35</b>
<b>1.10 Methods.....</b>	<b>36</b>
1.10.1 Cell Culture Method Protocols .....	36
1.10.2 The Protocol of Thawing, Culturing and Freezing Cell Line .....	36
1.10.3 Protocol of MTT Assays .....	37
1.10.4 Method Setup.....	39
1.10.5 Calculations and Evaluation of Obtained Absorbance Values .....	39
<b>1.11 Results and Discussion .....</b>	<b>40</b>
<b>1.12 Future Works.....</b>	<b>46</b>

<b>CHAPTER 2: HUMAN MESENCHYMAL STEM CELLS DIFFERENTIATION REGULATED BY NEAT ATSP AND COMPOSITE ATSP (%10 HYDROXYAPATITE CONTENT WITHIN ATSP) .....</b>	<b>48</b>
<b>2.1 Introduction .....</b>	<b>48</b>
<b>2.2. Materials .....</b>	<b>50</b>
2.2.1 Foam Samples.....	50
<b>2.3. Cell Culture, Assay, and Imaging Protocols.....</b>	<b>50</b>
2.3.1. hMSC culture and differentiation protocol .....	50
2.3.2. MSC thawing and counting procedure .....	51
2.3.3. MSC passaging procedure .....	52
2.3.4. MSC freezing procedure .....	52
<b>2.4. Quantification of MSC metabolic activity .....</b>	<b>53</b>
2.4.1. Ethylene Oxide Sterilization of Scaffold.....	54
2.4.2. Scaffold hydration.....	54
2.4.3. Standard curve for alamarBlue® .....	55
2.4.4. Seeding cell on the scaffold .....	58
2.4.5. alamarBlue® Protocol .....	58
<b>2.5. RT PCR .....</b>	<b>59</b>
2.5.1 RT PCR Procedure .....	60
<b>2.6. Statistical analysis .....</b>	<b>68</b>
<b>2.7. Results and Discussion.....</b>	<b>68</b>
<b>2.8. Future Works.....</b>	<b>74</b>
<b>REFERENCES .....</b>	<b>75</b>

## LIST OF FIGURES

Figure 1.1 The structure of the discipline of biomaterials .....	2
Figure 1.2 The old biomaterials paradigm.....	3
Figure 1.3 The emerging new biomaterials paradigm.....	3
Figure 1.4 Chemical structure of ATSP monomers and oligomer.....	8
Figure 1.5 Reduction process of MTT into formazon using enzyme reductase .....	26
Figure 1.6 The absorbance wavelength of alamarBlue®.....	27
Figure 1.7 Foam sample of ATSP.....	29
Figure 1.8 Bulk Sample of neat ATSP.....	30
Figure 1.9 Bulk Sample of composite ATSP.....	30
Figure 1.10 Film sample of neat ATSP .....	31
Figure 1.11 Film sample of composite ATSP.....	31
Figure 1.12 SEM image of foam ATSP sample .....	32
Figure 1.13 SEM image of bulk ATSP sample.....	33
Figure 1.14 SEM image of film ATSP sample .....	33
Figure 1.15 Foam Micro-Ct ATSP sample .....	34
Figure 1.16 Micro-Ct Images of Foam ATSP sample .....	35
Figure 1.17 Example of Micro-Ct Image used in Porosity Calculation .....	35
Figure 1.18 The steps of the MTT assay.....	38
Figure 1.19 Arrangements of the material samples inside the 6-well plate.....	39
Figure 1.20 The reduction of MTT to formazon.....	40
Figure 1.21 Cell viability results of neat bulk samples by MTT .....	41
Figure 1.22 Cell viability results of composite bulk samples by MTT .....	42
Figure 1.23 Cell viability results of neat film samples by MTT.....	43
Figure 1.24 Cell viability results of composite film samples by MTT .....	43
Figure 1.25 Cell viability results of neat foam samples by MTT .....	44
Figure 1.26 Cell viability results of composite foam samples by MTT .....	44
Figure 2.1 The schematic of alamarBlue® Plate .....	53
Figure 2.2 from left to right; composite (ATSP+HA) with osteogenic growth media (COM), composite (ATSP+HA) with regular growth media (CGM), scaffold (neat ATSP) with osteogenic media (SOM), scaffold (neat ATSP) with regular growth media (SGM) .....	55
Figure 2.3 Day 0- alamarBlue® standard curve plate .....	55
Figure 2.4 The alamarBlue® reduction into standard plate.....	57
Figure 2.5 The schematic of TaqMan test protocol .....	60
Figure 2.6 NanoDrop Lite.....	64
Figure 2.7 The metabolic activity of foam samples with alamar blue by MSCs.....	69
Figure 2.8 The results of SSP1 expression .....	71
Figure 2.9 The results of IBSP expression.....	72
Figure 2.10 The results of RUNX2 expression.....	73

## LIST OF TABLES

Table 1.1. The Basic Mechanical and Physical Requirements for the Design of Biomaterial .....	11
Table 1.2. The International Organization for Standardization (ISO) standards for biocompatibility testing. ....	16
Table 1.3. List of individual parts of ISO 10993 “Biological Evaluation of Medical Devices” ..	17
Table 1.4. Biocompatibility matrix, parts with relevance to this study are highlighted. ....	20
Table 1.5. The types of evaluation types and their test methods .....	22
Table 2.1. The calculations of alamarBlue® standard curve.....	56
Table 2.2. The calculations of percentage reduction of alamarBlue®.....	58
Table 2.3. Calculations for TaqMan .....	67

## CHAPTER 1: INTRODUCTION

### 1.1 Introduction

Synthetic materials have been used in the human body in previous studies. Polymer-based synthetic biomaterials have been progressively used in various therapeutic applications (mostly either as substitution or restoration of tissues and organs) because of their structural and mechanical properties [2]. They can also be engineered into different forms, shapes, and structures [3,4]. Besides, physical, chemical, and biological properties of synthetic polymers can be tuned to match the requirements of specific applications [5]. The adaptability of these polymers allows the design of new materials, structures and different forms with a variety in porosity, pore sizes, and mechanical properties. Also, engineered polymers can be effectively scaled-up compared to conventional polymers. Even though synthetic polymers do not have a functional group for stimulation of cell adhesion, they can bind to bioactive particles, such as hydroxyapatite (HA) or protein sequences, to activate particular cell reactions. [6] Therefore, synthetic polymers for biomedical applications have outweighed natural polymers and other bone substitute materials. However, broad biocompatibility assays of new materials should be performed, and new synthetic materials should be biocompatible for medical applications, with an absence of immunogenic reaction. Neither the polymer nor its degradation products should cause irritation or toxicity in-vivo because they can cause delivery of toxic chemicals. These chemicals may damage the cells in the neighboring tissue and affect negatively human health [7].

### 1.2 Biomaterials

The field of biomaterial is an interdisciplinary subject based on the engineering, pharmaceutical, physical, and biological sciences [8]. In general, biomaterials are characterized

as any synthetic or natural substance, aside from nourishments and vitamins, which are suitable for utilization as a framework for treatment or substituent for any tissue and organ. Biomaterials need to fulfill various essential criteria before they can be utilized as a part of biomedical applications. Hence, biomaterials should be subjected to multiple tests as prescribed by different associations and protocols. These tests should be done to determine the proper utilization of materials and also decide their safety level for clinical applications in people [9].

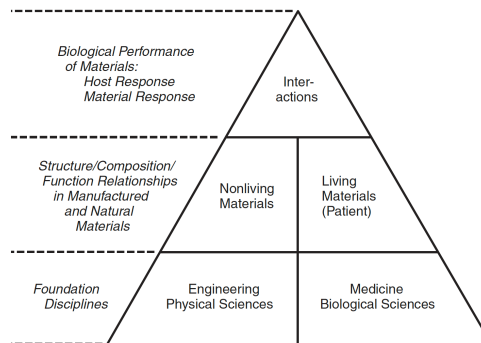


Figure 1.1 The structure of the discipline of biomaterials [10]

### 1.2.1 Concept of Biomaterials

Biomaterials began to be used inside the body in the mid-1970s. In the early investigations of the biomaterial for biomedical applications, the primary focus was to analyze the interface between the patient and the implant considering the material effect on the patient and local host reaction on the implant. Also, the examination of physical response of biomaterials like the fracture, wear, consumption, and disintegration were studied (Fig 1.2) [10].

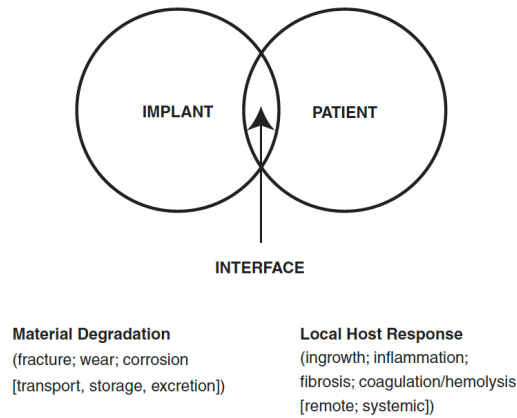


Figure 1.2 The old biomaterials paradigm [10]

As the field developed, primary interest moved far from the search for inert (class 1: inert) materials to bioactive (class 2: interactive) materials. The materials were changed by the design of three-dimensional structures over two-dimensional interfaces and patient by cell, and a third factor, signal, was added. Each of these factors communicates with the other two: the cells are influenced by the matrix and signals; the signals are altered by cell action and a matrix while the materials can be influenced by cells and signaling molecules [11].

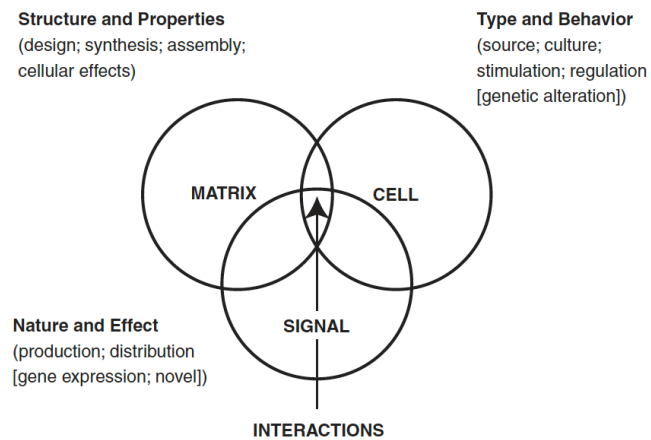


Figure 1.3 The emerging new biomaterials paradigm [11]



### 1.2.2 Types of Biomaterials

Biomaterials must have specific chemical, mechanical, physical, and biological properties prior to their first performance as biomaterials inside the human body. Hence, implant materials should show favorable response in a given biological system which carries out extremely complex functions. For instance, the pH values in different tissues differ from 1 to 9. During daily activities, the force experienced by the ligaments and tendons is around 40– 80 MPa, while bones are subjected pressure roughly 4 MPa. Moreover, these stresses are repetitive and depend on the activities (jumping, standing, jogging). For example, for one year period the stress cycles occurred by the finger joint motion or hip joint motion are estimated to be as high as  $1 \times 10^6$  cycles while it is  $0.5 \times 10^7$ – $4 \times 10^7$  cycles for a heart. This information roughly indicates the minimum and average numbers for biological environment where the biomaterials need to survive. Therefore, biomaterials are expected to be compatible with the biological systems. Hence, to meet certain standards, they are specifically developed neat or combined with classes of materials: polymers, metals, composite materials, and ceramics [12].

The classes of the materials are explained in the following sections:

Polymers are suitable materials for biological applications, especially in the replacement of various soft tissues and implants, such as cardiac valves, artificial hearts, and dental materials [13]. Also, polymer materials have many advantages compared to other materials including simplicity and ease in manufacturing with convenient mechanical and physical properties, and suitable cost. The desired features of polymers can be obtained by adjusting the formation, structure, and organization of constituent molecules, [14]. Furthermore, the manufacturing of polymers with different arrangements and compositions is required for its adaptability for various applications to satisfy specific requirements. These manufactured for biological

applications polymers are defined as synthetic polymers. Although there are some approved synthetic polymers for biological applications, the inadequacy of biocompatibility in most cases is the disadvantage. Because of this, their usage in medical applications may result in inflammatory reactions. These disadvantages can be altered by using natural polymers (such as chitosan, carrageenan, and alginate) and bioactive materials as fillers inside the synthetic polymer to increase biocompatibility [15].

Metals or metal alloys are the most preferred and demanded materials in the medical applications throughout history. The advantages of metals and metal alloys are their excellent biocompatibility, suitable mechanical properties, good corrosion resistance, and low cost [16]. In addition to this, their suitable tensile and fatigue strength make them perfect bearing materials compared to other classes of material such as polymers and ceramics. Furthermore, metals possess high toughness and elastic modulus but lower strains at failure compared to polymers. However, metals have relatively lower strength and higher toughness in comparison to ceramics. The choice of metals or metal alloys for the biomedical applications depends on the surrounding environment and its function. Their high tensile strength and fatigue limit make them good bearing materials compared to other classes of material such as polymers and ceramics. When the metal-based biomaterials are implanted into the body, the interactions between cells, tissues, and implanted material occur by the released by-products in consequence of changing and degrading of the surface of the biomaterial [14]. This factor enhances the understanding of the surface features of metal products to advance biocompatible materials. The stainless steel (316L), titanium and alloys (commercially pure Ti (Cp Ti), Ti6Al4V), cobalt chromium alloys (Co-Cr), aluminum alloys, zirconium niobium, and tungsten alloys are the most used metals as implants. The 316L type stainless steel (316L SS) is the most favored alloy in all implants from

cardiovascular to otorhinolaryngology applications. Co, Cr, and Mo alloys are preferred in need of high wear resistance for implant application such as artificial joints [10].

Composites are the combination of at least two or more substances with different physical and chemical properties. They are designed to have superior and distinctive properties from the components. These materials obtain three phases; i) matrix (continuous bulk phase), ii) reinforcement (composed at least one discontinuous dispersed phase and has better properties than the matrix), and iii) interphase (phase between the matrix and reinforcing elements). Composites are implemented in some specific applications in which tissue ingrowth is required. Also, their excellent features make them alternative candidates for load-bearing tissue components. Further, composites can be tailored for calcified tissue applications such as skull reconstruction and bone, knee, and ankle fracture repair. For example, cancellous bone-like composite porous scaffolds combined with bioglass fragments were engineered, which have similar mechanical features to the cancellous bone [10].

Ceramics are fundamentally inorganic, nonmetallic solids typically constituted at high temperatures. These materials are the specific class of biomaterials due to inertness in the body, high compressive strength, and excellent wear characteristics. The designed ceramic biomaterials for the biomedical applications are utilized in the musculoskeletal system, hip prostheses, artificial knees, bone grafts, and dental and orthopedic implants. Also, they are used as coatings on the surface of metallic implants to enhance their biocompatibility. Despite these criteria, their biomedical applications are less than metals and polymers because of their brittleness and low tensile strength. Hence, the phosphate bio ceramics are engineered and designed to overcome the brittleness and low tensile strength of the conventional ceramic biomaterials which have high biocompatibility and bone reconciliation, and also, they have a similar structure of the mineral

part of the bones [13]. The calcium phosphate-based biomaterials are utilized for various distinctive applications through the body, encompassing all territories of the skeleton. A couple of its applications are dental inserts, joint substitution, orthopedics, and treatments. Second, hydroxyapatite has been utilized as a filler in the bone imperfections and as implants in nasal septal bone [17]. It is also utilized as a coating on titanium, stainless steels, and metallic orthopedic and dental inserts to advance their affinity to the bone [18].

#### 1.2.2.1 Aromatic Thermosetting Copolyester (ATSP)

Aromatic thermosetting copolyester (ATSP) is known as a cross-linkable aromatic polyester oligomer which was first produced by Frich et al. [19]. In the 1990's, Prof. James Economy at University of Illinois at Urbana-Champaign advanced the ATSP research. The synthesis of the ATSP was done in two steps by controlling the molar ratios of the oligomers composed of biphenol diacetate (BPDA), 4-acetoxy benzoic acid (ABA), isophthalic acid (IPA), and trimesic acid (TMA). In the reaction, carboxylic acid and acetoxy end group were incorporated by an endothermic condensation method. Biphenol diacetate (CB and CB<sub>2</sub>) was used in the carboxylic acid end group while acetoxy end group had biphenol diacetate (AB and AB<sub>2</sub>) where "2" symbolize numeration (Fig. 1.4).

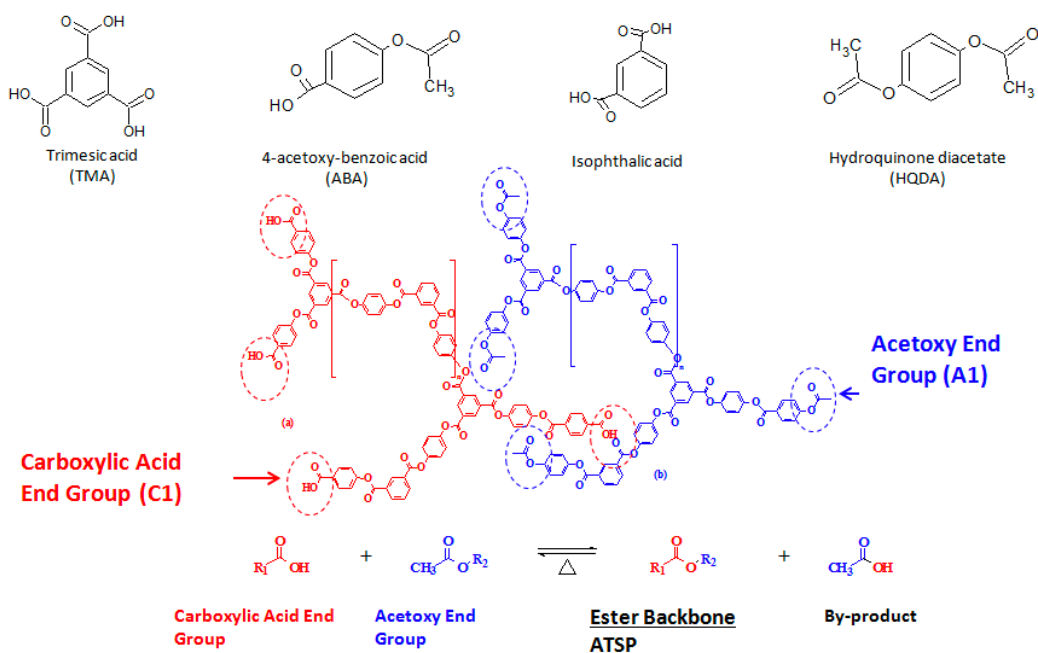


Figure 1.4 Chemical structure of ATSP monomers and oligomer [20]

The bulk aromatic thermosetting copolyester (ATSP) with the density of  $1.27 \text{ g/cm}^3$  for CBAB were produced by the following procedure: (i) blending ATSP oligomers ( $<90 \text{ um}$ ), (ii) curing the blend to produce foam, (iii) grinding the cured material to a powder, (iv) sintering of the cured powers via hot press. ATSP foams were produced by the same oligomer groups by entrapping acetic acid inside ATSP and the blowing agent (acetic acid) which formed a macro cellular porous structure inside the polymer matrix [20]. Also, the rigid rod structures have the poor solubility on any solvent; however, the branch structure of the ATSP enhances the solubility and allows ATSP to be produced into thin films. To obtain thin films, the solution of carboxyl and acetic acid end group oligomer in N-methyl-2-pyrrolidinone (NMP) was used and poured on the aluminum foil. During the curing process, no force nor vacuum were applied. The composed films were separated from aluminum by submerging the foil in concentrated hydrochloric acid (HCl) for seconds. The following steps involved washing the film with

deionized water and overnight drying process in the oven [21]. The composite ATSP polymers were produced by blending ATSP oligomers with 10% weight (wt.) hydroxyapatite (HA) and the same bulk, film and foam procedures were followed.

ATSP has advantageous properties including low cost and ease in manufacturing. ATSP demonstrates excellent mechanical properties, especially in strength and stiffness. Besides, it demonstrates advantageous features as adhesives, matrices for composites, and coatings with low friction coefficient, excellent wear, and abrasion resistance. Their cross-link structures cause the inertness and stable properties. In addition to this, having robust adhesive features with metals, high energy absorption limit, and promising tribological properties make the ATSP a strong candidate for different orthopedic implant applications [20].

### 1.2.3 Characterization of Biomaterial

A biomaterial should have essential qualities to be used efficiently as a material inside the body. These qualities are specified beneath.

- Nontoxicity:

A biomaterial should be nontoxic inside the body and should not influence other organs and tissues. The toxicity can be defined as harmful leachable which segregates out of the material. Therefore, the nontoxic materials have no carcinogenic, pyrogenic, allergenic, and inflammatory responses [22].

- Biocompatibility:

All biomaterials which are used in the body experience tissue reactions; therefore, biocompatibility is commonly characterized as the ability of a biomaterial to interact positively during a particular application. "Suitable host reaction" incorporates absence of blood clotting,

inflammatory response, and protection of bacterial colonization. Thus, the biomaterial is required to be biocompatible to work appropriately in patient's body [23].

- An absence of Foreign Body Reaction:

The responses created by the existence of a different substance in a human body are implied as a "foreign body reaction." This response will be different in intensity and period depending on the anatomical site. Therefore, biomaterials should execute all the criteria as proposed in the universal protocols and introduce no critical damage to the patient. The biomaterial should demonstrate no foreign body response [22].

#### 1.2.4 Mechanical Properties and Performance of Biomaterials

The coordinating of biomaterial physical properties with the vital organ/tissue properties is the most critical requirement. Biomaterials should have reasonable mechanical and performance features which are comparable to the supplanting organ/tissue. Subsequently, the materials should be designed considering the tissue environment where the devices will be utilized. The essential mechanical and physical requirements for the new biomaterial are mentioned under three titles specified below [23]:

##### 1.2.4.1 Mechanical performance

One of the significant challenges in the biomaterial field is producing biomaterials with adequate mechanical properties. Mechanical performance of a biomaterial should show the proper and expected properties in the living body. The mechanical standards for the biomaterial fluctuate depending upon the site of utilization. For example, biomaterials, which are characterized by high mechanical stiffness and high strength, should be employed for applications where more mechanical support is needed such as hip joints. However, biomaterials that are preferred in the hip joint are entirely unacceptable for the use as artificial heart valves

which require biomaterials with more compliant elastic features than hip joint substitute materials. The mechanical performance of some biomaterials is represented in Table 1 [23].

#### 1.2.4.2 Mechanical durability

Durability shows the shortest time of duration of the material inside the body up to the longest duration time when a biomaterial adequately achieves its expected capacity. Clearly, a heart valve must be able to flex without tearing for a lifetime. The mechanical span of some of the biomaterials is specified in Table 1 [23].

#### 1.2.4.3 Physical properties

Biomaterials should have a particular physical property with a specific performance to achieve its desired behavior. Table 1 demonstrates the required physical properties for various biomedical applications [23].

Table 1.1. The Basic Mechanical and Physical Requirements for the Design of Biomaterial [23]

Mechanical Performance	
Biomaterial	Mechanical Characteristics
Hip prosthesis	Strong and rigid
Tendon material	Strong and flexible
Heart valve leaflet	Flexible and tough
Articular cartilage	Soft and elastomeric
Dialysis membrane	Strong, flexible, and nonelastomeric
Mechanical Durability	
Biomaterial	Mechanical Durability
Catheter	3 days
Bone plate	6 months or longer
Leaflet in heart valve	Must flex 60 times per minute without tearing for the lifetime of the patient
Hip joint	Must function under heavy loads for more than 10 years
Physical Properties	
Biomaterial	Physical Characteristic
Dialysis membrane	Permeability
Articular cup of the hip joint	High lubricity
Intraocular lens	Clarity and refraction



### 1.2.5 History of Biomaterials

The first synthetic biomaterials embedded into the human body were utilized many centuries ago. For example, a biomaterial was present in the remains of the human skeleton of a prehistoric Paleoamerican man found near Kennewick, WA (often referred to as the “Kennewick Man”). The spear point about 9000 years old was located in the hip of the body. Also, scientists discovered gold wires which were utilized to link loose teeth in ancient Phoenicia. Furthermore, Mayan people used seashells to design nacre teeth in roughly 600 AD. The bone integrated iron dental implant was found in a corpse in 200 AD. In the early 20<sup>th</sup> century, bone plates were proposed to treat the fixation of long bone fractures. However, their mechanical design was not adequate for stress bearing because the structure was too thin, and stress was concentrating on corners. Instead, vanadium steel was chosen because of its good mechanical properties, but it caused both corrosion in the body and adverse effects on the healing processes. Therefore, better designs and materials were needed. The expected achievement was succeeded by stainless steels and cobalt-chromium alloy in terms of fracture fixation and the first joint replacement. Like metals, polymers, particularly poly (methyl methacrylate), were widely preferred for replacements of sections of damaged skull bones. With the further advancements in materials and surgical techniques, blood vessel replacements were tried in the 1950s. During the 1960s heart valve replacements and cemented joint replacements came into usage. At the beginning of the twenty-first century, biomaterials were broadly employed in medicine, dentistry, and biotechnology [23].

### 1.3 Biocompatibility

The improvement in biocompatible materials began in the late 1960s with the acknowledgment that synthetic items could be adequately used as a part of the body. Although

these improvements in the biocompatible materials were beneficial, they also brought many new challenges with safety, quality, and the mechanical competence of biomaterials for the body. Because of these challenges, inquiries frequently emerged concerning security and the mechanical properties of the material, and how such qualities could be fulfilled preceding the devices utilized as a part of human patients. Particularly, the most difficult issues were the reactions of the human body against biomaterials and the response of tissues to these materials. This subject was given the name 'biocompatibility' [24].

The term biocompatibility has encompassed the behavior of biomaterials in the living body. The thirteen most accepted definitions and terms of biocompatibility were decided by a consensus at the European Society for Biomaterials conference in 1986 [8]. In this conference, biomaterials were defined as “a material employed in a medical device which should interact with biological systems, while host response was described as the reaction of a living system to the presence of a material”. The ability of a material to have an appropriate host response in a specific situation was assigned as the definition of biocompatibility [8].

Although those definitions are widely accepted, the most well-known meaning of biocompatibility was done by D. F. Williams (2008): “Biocompatibility is referred as the function of a biomaterial to be performed its desired capacity regarding a medical therapy, the most appropriate cellular or tissue response in that specific situation, and optimizing the clinically relevant performance of that therapy apart from revealing any defective local or systemic effects in the receiver of that therapy.” According to this definition, all biomaterials independent of their performing area should show a biocompatible reaction. More generally, biocompatibility can likewise be characterized as the connection between a material and the living being with the goal of producing no bothersome impacts [23].

### 1.3.1 History of biocompatibility

The examples of "biocompatibility" have been seen throughout history. The male body with a biocompatible spear point in pelvis dated 8000 years back was found in the territory of Washington (United States), close to the town of Kennewick. It is believed that this man survived with that lance point in his body during a long period of his life. One reason could be that the lance point was surrounded by a collagenous capsule (the foreign body response, FBR), and it was detached from person's body like a contemporary implant [25]. In 1931, the skull of a Mayan woman dated 600 AD was found with three seashell dentals during an archaeological excavation in Honduras [26]. Wrought iron was used as a dental implant for an upper tooth in France in the period of AD 100–200, as uncovered by a radiological examination. Additionally, the radiological image showed that osseointegration was comparable to the current criteria for the dental implants [27]. In the 1890's, the implant materials began to be used. German specialist Themistocles Glück utilized ivory and nickel-plated equipment to design a hip prosthesis. At the same period, a Czech specialist Vitezlav Chlumsky explored the possibility of utilizing silver, magnesium, zinc, glass, plastic, and celluloid as hip joint interposition materials. British ophthalmologic specialist, Dr. Harold Ridley discovered that the pilots had unexpected implantations of windshield fragments in their eyes during World War II because of machine gunfire that broke airplane windshield into small pieces. The windshield was produced from poly (methyl methacrylate) (PMMA) and Dr. Ridley realized that the fragments which were embedded into pilot's eyes for few years had little inconvenience. Although Ridley never used the expression "biocompatibility," his perception of inertness and absence of negative response was long the present-day thoughts of biocompatibility. Subsequently, he used PMMA to make the first human intraocular lens (IOL), with the first implantation done in 1949 [28].

The expression "biocompatibility" was developed around 1970, in a fundamental paper by C.A. Homsy, where the ideas of toxicology and its relationship to biocompatibility were elucidated [29]. In 1971, Homsy's thoughts were coordinated into a progression of tests to survey the appropriateness of materials for National Institutes of Health (NIH) [30].

### 1.3.2 Selection of biocompatibility analyses

The approved and accepted biocompatibility assays are separated into three categories: essential (level I), secondary (level II), and preclinical (level III) tests. These groups include the cytotoxicity examination and irritating capability of entire systems in animals within muscular implants, skin implants, or in culture systems. Since the ATSP is a recently introduced material, in-vitro Level I tests will be the focus for the cytotoxicity tests of ATSP. In-vitro Level I assays evaluate the material properties in cultured cells environment to determine materials' toxicity [31]. Since international standards and protocols provide documents which help in designing an appropriate test protocol, specialists should adhere to universal standards including Food and Drugs Organization (FDA) direction, ISO 10993: "Biological Evaluation of Medical Devices", or The European standards EN 30993. Table 2 records the ISO principles for biocompatibility tests. The tests which are suggested for examining the biocompatibility or on the other hand biological impacts can be categorized as below [32]:

- (A) Cytotoxicity or cell viability
- (B) Sensitization
- (C) Irritation
- (D) Acute systemic toxicity
- (E) Subchronic toxicity
- (F) Genotoxicity

(G) Implantation

(H) Hemocompatibility

(I) Biodegradation.

Table 1.2. The International Organization for Standardization (ISO) standards for biocompatibility testing [32].

**ISO standards for biocompatibility tests**

ISO standards	Title	Description
ISO 10993 ISO 10993-1:2009	Biocompatibility Evaluation and testing in the risk of management process	It describes basic guidelines of biocompatibility It describes general principle governing the biological evaluation of medical devices within a risk management process. It also includes general categorisation and duration of the contact
ISO 10993-3	Tests for genotoxicity, carcinogenicity, and reproductive toxicity	The standard specifies strategies for hazard identification and tests on medical devices for the following biological aspects: genotoxicity, carcinogenicity, and reproductive and developmental toxicity
ISO 10993-4	Selection of tests for interactions with blood	The standard provides a general requirement for evaluation of the intersections of medical devices with blood.
ISO 10993-5	Tests for in vitro Cytocompatibility evaluation	The standard describes test methods to assess the in vitro Cytocompatibility evaluation of medical devices. These methods specify the incubation of culture cells in contact with a device and extracts of a device either directly or through diffusion
ISO 10993-10	Tests for irritation and delayed-type hypersensitivity	The standard describes the procedure for the assessment of medical devices and their constituent materials about their potential to produce irritation and skin sensitisation.
ISO 10993-11	Tests for systemic toxicity	The standard specifies requirements and gives guidance on procedures to be followed in the evaluation of the potential for medical device materials to cause adverse systemic reactions
ISO 10993-18	Chemical characterisation of materials	Biological evaluation of medical devices Part 18: Chemical characterisation of materials
ISO 10993-19	Physicochemical, morphological, and topographical characterisation of materials	Biological evaluation of medical devices Part 19: Physicochemical, morphological, and topographical characterisation of materials

Table 1.3. List of individual parts of ISO 10993 “Biological Evaluation of Medical Devices” [31]  
(parts with relevance to this study are highlighted)

Part	Title
1	Evaluation and Testing
2	Animal Welfare Requirements
3	Tests for Genotoxicity, Carcinogenicity, and Reproductive Toxicity
4	Selection of Tests for Interactions with Blood
5	Tests for In-Vitro Cytotoxicity
6	Tests for Local Effects after Implantation
7	Ethylene Oxide Sterilisation Residuals
8	Selection and Qualification of Reference Materials for Biological Tests
9	Framework for Identification and Quantification of Potential Degradation Products
10	Tests for Irritation and Delayed-Type Hypersensitivity
11	Test for Systemic Toxicity
12	Sample Preparation and Reference Materials
13	Identification and Quantification of Degradation Products from Polymeric Medical Devices
14	Identification and Quantification of Degradation Products from Ceramics
15	Identification and Quantification of Degradation Products from Metals and Alloys
16	Toxicokinetic Study Design for Degradation Products and Leachables
17	Establishment of Allowable Limits for Leachable Substances
18	Chemical Characterization of Materials
19*	Physico-Chemical, Mechanical and Morphological Characterization
20*	Principles and Methods for Immunotoxicology Testing of Medical Devices

\*: under development

Cytotoxicity tests are the cellular level experiments that identify the toxic capability of a material or device [33]. These assays are sensitive, cheap, and the obtained outcomes are qualitative, quantitative, and practically comparable. The results permit the assessment of harmful materials prior to animal testing. Sensitization, also called allergic contact dermatitis, is a cutaneous reaction mediated by the immune response. It can be caused by periodic or continuous exposure to even a small amount of toxins. A sensitization response is shown as redness and swelling of the skin. Unfortunately, there is no settled in-vitro substitute assays [34].

In the Irritation test, the response is caused by chemicals discharged from devices or materials that contact the skin, eye, or mucous layer. Such irritation is defined as a local tissue reaction which is diagnosed by the indications of infection: redness, swelling, and fever [34].

The Acute Systemic Toxicity occurs because of the diffusion of chemicals from the material into the body where the substances may either positively or negatively affect organs or tissues within 24 hours after a dose [35].

The Subchronic Toxicity test is very similar to the Acute Systemic Toxicity test. The only difference is the testing time period which varies between 24 hours and 10% of the total life expectancy of the animal (for instance up to 90 days in rats) [35].

The Genotoxicity test examines the tendency of a medical device to prompt changes in the DNA structure of cells. There are three kinds of impacts, which should be tested independently: a) Gene changes, b) Changes in the chromosome structure, and c) DNA impacts. At least two of these tests should be performed in-vitro with mammalian or non-mammalian cells, microscopic organisms, yeast, or parasites [36]

Implantation tests are essential to evaluate the local impacts of the implants on surrounding tissues [37]. Implantation can prompt constant irritation, with degeneration, and tumor development in the neighboring tissue [36].

The chemical leakage from a device can cause the undesired changes in the blood, such as a formation of hemolysis or thrombus. The Hemocompatibility test allows to check whether the device leads to changes in the blood [38].

The Chronic Toxicity test is fundamentally the same as the Acute Systemic and Sub Chronic Toxicity test, but the exposure time is higher than 10% of the life expectancy of the animal [35].

The Carcinogenicity test decides the tumorigenic capability of a device by presenting it to the animal throughout its lifetime. The Reproductive and Developmental Toxicity test assesses

the potential impact of the device on reproductive capacity, embryonic advancement, and pre-birth and early postnatal improvement [36].

Biodegradation assays investigate the procedures of absorption, distribution, biotransformation, and disposal of leachable and degradation of items produced by the material segments of the device [39].

#### 1.4 Test Programs and Descriptions

The tissue environment where the material will be used and the residence time of material inside the body are primary criteria for selecting the reasonable test program. Hence, the requirements and the necessities for the different materials for different conditions will vary. For example, surface devices are intended to be in contact with skin temporarily for 24 hours, whereas an implant, which will stay longer than surface devices, has different necessities to be named biocompatible [40].

Therapeutic devices can be categorized as Table 2, and the required and conducted tests for ATSP are labelled to accomplish a certification of biocompatibility. These essential experiments should be accepted as a guideline; however, each device is unique so some tests are not practical or extra tests, which are not demonstrated in the table, should be conducted. Therefore, the historical background of utilization of ATSP or reported assays of material for biocompatibility should be considered [40].



Table 1.4. Biocompatibility matrix [40], parts with relevance to this study are highlighted.

DEVICE CATEGORIES			BIOLOGICAL EFFECT										
BODY CONTACT		CONTACT DURATION	Cytotoxicity	Sensitization	Irritation/Intracutaneous	Acute Systemic Toxicity	Subchronic Toxicity	Genotoxicity	Implantation	Hemocompatibility	Chronic Toxicity	Carcinogenicity	Reproductive/Developmental
		A = Limited (≤24 Hours)  B = Prolonged (24 Hours - 30 Days)  C = Permanent (>30 Days)											
SURFACE DEVICES	Skin	A	x	x	x								
		B	x	x	x								
		C	x	x	x								
	Mucosal Membrane	A	x	x	x								
		B	x	x	x	o	o		o				
		C	x	x	x	o	x	x	o		o		
	Breached or Compromised Surfaces	A	x	x	x	o							
		B	x	x	x	o	o		o				
		C	x	x	x	o	x	x	o		o		
EXTERNALLY COMMUNICATING DEVICES	Blood Path, Indirect	A	x	x	x	x				x			
		B	x	x	x	x	o			x			
		C	x	x	o	x	x	x	o	x	x	x	
	Tissue/Bone/Dentin Communicating¹	A	x	x	x	o							
		B	x	x	x	x	x	x	x				
		C	x	x	x	x	x	x	x		x	x	
	Circulating Blood	A	x	x	x	x		o²		x			
		B	x	x	x	x	x	x	x	x			
		C	x	x	x	x	x	x	x	x	x	x	
IMPLANT DEVICES	Tissue/Bone	A	x	x	x	o							
		B	x	x	x	x	x	x	x				
		C	x	x	x	x	x	x	x		x	x	
	Blood	A	x	x	x	x	x		x	x			
		B	x	x	x	x	x	x	x	x			
		C	x	x	x	x	x	x	x	x	x	x	x
<div>X = Tests per ISO 10993-1</div> <div>O = Additional tests that may be applicable in the U.S.</div> <div>Note¹ - Tissue includes tissue fluid and subcutaneous spaces</div> <div>Note² - For all devices used in extracorporeal circuits</div>													

#### 1.4.1 In-vitro cytotoxicity assays (ISO 10993-5:2009)

In-vitro cytotoxicity tests are well defined in ISO 10993-5 (ISO 10993- 5:2009) and are generally and regularly utilized for the assessment of biomaterials/medical equipment. The standard incorporates a timetable for testing which helps to decide the most proper assays for therapeutic devices [41]. Cytotoxicity tests have many advantages for toxicity assessment of therapeutic devices because they provide sensitive results and realistic estimate of toxicity and also decrease the number of animals used in cytotoxicity assays. The cytotoxicity test is one of the assessment and screening tests that utilizes tissue cells in-vitro to monitor the cell development, differentiation, and morphological impacts of medical equipment. Three sorts of

cytotoxicity test are in the International Organization for Standardization 10993-5: Extract, direct contact, and indirect contact tests [42].

The direct contact test is fundamental for the materials/material parts that will individually confront the body cells. In this test setup, the surface structure and the chemical compound of the material or device may impact the cells.

There are two potential applications for the direct contact test to analyze the material with cells: a) The cells are grown onto the material, or b) The cells are grown into a test vessel and the material is set over the cells [43].

An indirect contact test is designed to ensure that the surface properties are not affecting the outcomes. In this experiment, the cells and the material are isolated by an interface layer. The interface can be an agar-gel or a porous film. Hence, only dissolvable substances flowing out of the material can diffuse via the layer and cause cytotoxicity [43].

In the Agar Diffusion Test, materials which cannot react with agar can be used as a test material. Cells are seeded into the well plate, and culture medium layer with dissolved agar (0.5 to 2% weight (wt.) is pipetted over them. After solidification, the sample can be set over the cell layer [28].

In the Extract Test, the extract of the material is added in different concentrations to the cell culture to assess its toxicity quality. The most common media are physiological saline, culture medium, dimethyl sulfoxide, polyethylene glycol, or vegetable oil. The extraction of a material is a complicated procedure influenced by parameters like the extent of the reaction, temperature, and class or surface area of the material [43].

## 1.4.2 Cytotoxicity Evaluation Methods

The various characteristics and functions of the cell can be observed in the midst or after the cytotoxicity test [42, 43]. These properties can be classified into four different types of assessments: a) Change in cell morphology, b) Cell growth (proliferation), c) Cell viability, and d) Enzyme action of cells.

### 1.4.2.1 Cell Morphology

To analyze cell morphology, either a light-optical and scanning electron microscopy or staining can be employed. The inspection of the cells should be done microscopically before the cytotoxicity test starts and before it is completed. Changes in morphology, differentiation, separation, or cell lysis should be recorded. The most customarily utilized methods are shown in Table 3, and the alamarBlue® and the MTT are clarified in more detail with regards to their utilization in this thesis [44].

Table 1.5. Types of evaluation and their test methods [44]

<b>Evaluation Type</b>	<b>Tests</b>
Cell Proliferation	Colony Formation
	<sup>3</sup> H-Thymidine Incorporation
	BrdU Incorporation
	Detection of Antigens/Antibodies
Cell Viability	Cell Count (Haemocytometer)
	<sup>51</sup> Cr Release
	Trypan Blue Exclusion
	Neutral Red Uptake
	Crystal Violet Inclusion
Enzyme Activity	LDH Release
	Reduction of Tetrazolium Salts (MTT, XTT test)
	Oxidation-Reduction Activity (alamarBlue™)

#### 1.4.2.2 Cell Proliferation

The proliferation term is defined as a cell division which estimates the quantity of dividing cells in culture. The Colony Formation test is the least complicated technique to quantify the proliferation. A specific number of cells that are plated into an appropriate size flask is the first step for this assay. This step is followed by the counting of the number of colonies after the determined time points (after one day, two weeks or three months). However, this strategy is not easy for a significant number of samples [44]. Also, the markers like  $^3\text{H}$ -Thymidine or 5-Bromodeoxyuridine (BrdU) can be fused into the DNA to gauge the DNA synthesis. These strategies give exact estimates. However, when many samples (immunohistochemistry) are required, the number of samples can create ambiguity in the results. The Detection of Antigens/Antibodies is a correct strategy when it comes to the observation of particular antigens or antibodies, which are present in proliferating cells [44].

#### 1.4.2.3 Cell Viability

The number of healthy cells can be used to define the cell viability. It is hard to distinguish if the cells are dividing or are inactive. Therefore, culturing and utilizing no dividing cells (primary cells) will be more favorable. Determining the number of alive cells can be done by counting them in the hemocytometer. Since this straight calculation has a risk of an error, it is not useful for a large number of samples. Therefore, indirect methods for counting the number of cells are preferred. Some of the indirect cell counting for cell viability techniques are [44] as described next.

Radioactive chromium markers are fused into cells in the  $^{51}\text{Cr}$  Release test where the living cells hold this marker while the dead cells discharge the radionuclide into the medium. The scintillation counting is used to estimate the release and to distinguish the resultant light

pulse. This test has a few drawbacks including expenses, essential equipment, and safety prerequisites related to the treatment of radioactive materials [44].

The Trypan Blue Exclusion test is fast and simple to perform when analyzing the viability of cells. This assay depends on the absorption or exclusion of dye, which only dyes the dead cells because the non-harmful dye cannot saturate in the intact cell membranes. This test is regularly combined with counting cells in a Hemocytometer to recognize living and dead cells [44].

The Neutral Red Uptake technique allows to stain only viable cells as cells absorb the dye in their lysosomes. After washing the cells, subsequently they will extract the dye and the absorbance of the dye which is proportional to the viable cells measured by a spectrophotometer. The absorbance of the dyed cells can be estimated spectrophotometrically at around 550 nm [45]. The Crystal Violet Inclusion identifies the cell lysis. The dye only stains the living cells, which stick to the surface of cell culture flasks. At the point when cells experience lysis, they disengage from the surface. The living cells which absorbed the dye are distinguished spectrophotometrically.

Lactate Dehydrogenase (LDH) is an enzyme existing in the cytoplasm of all cells. This enzyme is quickly flown out into the cell culture medium when the plasma membrane gets harmed. The LDH action can be efficiently estimated with samples obtained from the medium at a specific period. The enzymatic response involves two stages. First, discharged LDH are reduced  $\text{NAD}^+$  to  $\text{NADH} + \text{H}^+$  by oxidation of lactate to pyruvate. Second, the impetus (diaphorase) exchanges  $\text{H}/\text{H}^+$  from  $\text{NADH} + \text{H}^+$  to the yellow tetrazolium salt, which is a reduction of the yellow tetrazolium salt to red formazan. An increase in the amount of the LDH catalyst in the medium is due to a rise in the number of cells with a damaged membrane, and this

corresponds to the amount of formazan salt composed in a particular and constrained time frame. In this way, the quantity of dye generated in the test is proportional to the number of lysed cells. The formed formazan is a soluble dye in a culture medium and demonstrates absorption, most extreme near 550 nm [46].

#### 1.4.2.4 Enzyme Activity

3, (4,5-dimethyl-thiazol-2-Yl)-2, 5-diphenyltetrazolium bromide [MTT], the most broadly approved cytotoxicity test among other cytotoxicity assays, was introduced by Mossman in 1983. He utilized this semi-automated, colorimetric assay to quantify cytotoxicity, proliferation, and activation in lymphocytes [47]. The tetrazolium salt model presented by Mossman has been utilized broadly to recognize viable cells [49]. After Mossman published the paper, the article not only lead to broad utilization and approval of this assay but also helped to discover and solve non-disintegration of the formazan color. It also empowered the improvement of other scaled down, semi-automated, colorimetric tests like the LDH 96 well assay. Also, the test was tried on a broad scope of human cell lines, and in most cases, alive cell number were proportional to formazan generation [48]. Throughout the years, the MTT-based test is a standout amongst the other cytotoxicity assays in malignancy exams in cancer research for assessing cell viability, proliferation, and medication cytotoxicity. It can also be used for proliferation and cytotoxicity tests [49].

MTT [3, (4,5-dimethyl-thiazol-2-yl)-2, 5-diphenyltetrazolium bromide], a water soluble yellow color solvent, is changed by the chemical succinate dehydrogenase in the mitochondria of metabolically active cells into a dark purple insoluble formazan item [47]. The enzyme reduction happens through its lipophilic side of cell membrane, and the positively net charged water soluble yellow solvent (MTT) can pass through the cell membrane. It is then reduced in

viable cells by mitochondrial or cell plasma proteins like oxidoreductases, dehydrogenases, oxidases, and peroxidases (Fig. 1.5). This reduction causes a transformation of a water-soluble tetrazolium salt to the water-insoluble formazan (dark purple color). The water insoluble purple formazan is able to be solubilized by dimethyl sulfoxide (DMSO), which is generally used to solve the formazan product [48]. The absorbance of dissolved formazan product is able to be measured between 570 and 590 nanometers (nm) via a plate reader [47].

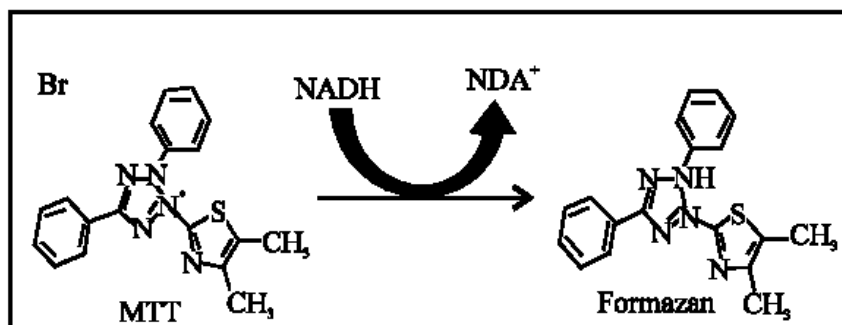


Figure 1.5 Reduction process of MTT into formazon using enzyme reductase [50]

The alamarBlue® Assay is the quantitative measurement of the proliferation of different human and animal cell lines. The assay is a colorimetric technique for the identification of the metabolic action of cells and is utilized to discover a relative cytotoxicity of different substance [51].

The technique depends on the reduction of resazurin (blue dye) and the fluorescent, colorimetric agent resorufin (pink dye) by metabolically active cells that allow diaphorase action [52]. This reduction results in change from non-fluorescent indigo blue to fluorescent pink state. The alamarBlue® reduction is examined by estimating either the fluorescence or the absorbance spectrophotometrically at two wavelengths 570 and 600 nm (Fig. 1.6). The fluorescent signal is

proportional to the number of live cells; thus, it allows an accurate quantification of changes in the rate of cell proliferation and day by day observation of the enzymatic movement of the cells [53].

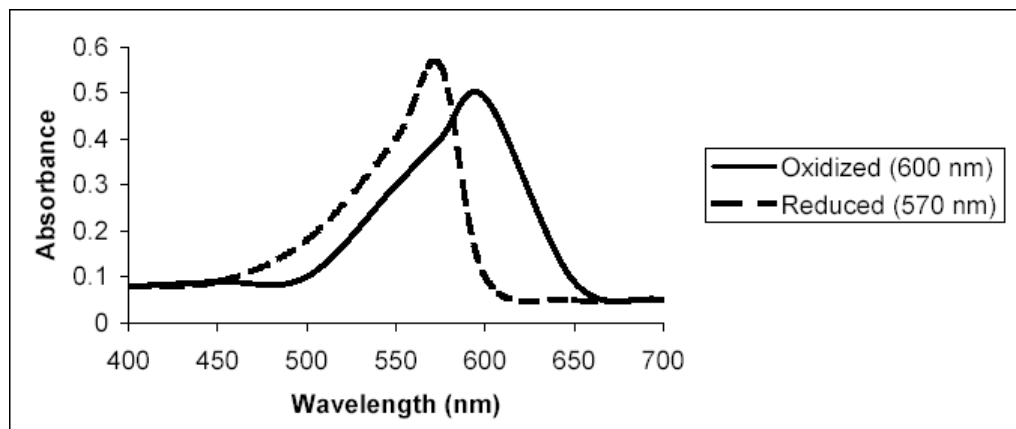


Figure 1.6 The absorbance wavelength of alamarBlue® [54]

### 1.5 Experiment Setup for ATSP

As clarified at the beginning of section 2, biocompatibility is not only based on the effect of neighboring cells or tissue but also the expected functionality of the materials; therefore, a proper test setup should be performed by considering these two criteria. The assay should be simple, reproducible, and precise. Hence, the cytotoxicity assay was selected for this research since cytotoxicity tests are the initial step of the in-vitro biocompatibility analysis, and this test gives quantitative and similar results to the results of in-vivo assays. The tetrazolium-based MTT test was explicitly chosen for the cytotoxicity assay because it is accepted as the most sensitive and used as a high-throughput screening test. The principle of colorimetric MTT assay depends on the mitochondrial dehydrogenase action of viable cells. This test measures the metabolic cell activity by the result of an enzymatic transformation of the tetrazolium compound to water-insoluble formazan by dehydrogenases, which happens in the mitochondria of living cells. In terms of cell line, human osteoblast cells were used in this experiment for cytotoxicity assays.



These cell lines are generally preferred and utilized for the initial step of cytotoxicity testing for bone implant materials. Also, they are easy to handle in culture and the results are accepted as proportional to in-vivo results. The MTT assay with human osteoblast and skeletal cell lines are the most suitable assays for ATSP because it is still in its improvement stage, and the neat and composite ATSP are not yet confined to a specific application or a body condition [55].

## 1.6 Materials and Methods

### 1.6.1 Foam Samples

The endothermic condensation polymerization reaction occurred between aromatic based acetoxyl and carboxylic acid end-group oligomers. This reaction resulted in self-generated acetic acid that produced macro cellular porous morphology inside cross-linked ester backbone polymer lattice. ATSP foam samples were produced 6 mm in diameter and 4 mm in height with 70% porosity (Fig. 1.7). Three different weights, 35 mg, 70 mg, and 105 mg, were measured by the precision balance in mg, and they were studied with the same amount of cell density to analyze the concentration effect on cell metabolic activity. The samples were sanded by 100- 240 grit-sized sandpaper to reach the desired weight of 35 mg, 70 mg, and 105 mg. In addition to that, to produce the composite samples, the oligomers were mixed with 10% weight (wt.) HA before the process. The same procedure above was followed to produce the composite ATSP.



Figure 1.7 Foam sample of ATSP

#### 1.6.2 Bulk samples

Bulk samples of the ATSP were produced in four steps: (i) blending ATSP oligomers which was followed by (ii) curing the blend to create foam, and finally, (iii) the cured material was ground to a powder. At the next step, the cured powers were sintered through a hot press. The samples were cut into appropriate sizes  $3 \times 3 \times 3 \text{ mm}^3$  (Fig. 1.8) and bulk samples were again sanded by 100- 240 grit-sized sandpaper to get final weights of 35 mg, 70 mg, and 105 mg. Composite bulk samples were produced by adding 10% wt. HA to the oligomers and blending ATSP oligomers with HA, curing the blend to create foam, grinding the cured material to a powder, and sintering of the cured powers via the hot press (Fig. 1.9).



Figure 1.8 Bulk Sample of neat ATSP



Figure 1.9 Bulk Sample of composite ATSP

### 1.6.3 Film sample

The branched structure of ATSP enhances the solubility and allows ATSP to be produced as thin films. Film samples were created by pouring the solution carboxyl and acetic acid end group oligomer in N-methyl-2-pyrrolidinone (NMP) on the aluminum foil (Fig 1.10 and 1.11). For the composite films, 10% wt. HA was added to the oligomers in NMP, and the solution was poured onto the aluminum foil. During the curing process, no force or vacuum were applied to the neat and composite samples. Then, the neat or composite films which were deposited onto aluminum were separated from the aluminum foil by submerging it in concentrated hydrochloric acid (HCl) for seconds. The following step involved washing the film with deionized water and an overnight drying process in the oven [21]. The films were then cut and weighted as 35 mg, 70 mg, and 105 mg.



Figure 1.10 Film sample of neat ATSP



Figure 1.11 Film sample of composite ATSP

## 1.7 Sterilization of Samples

All of the samples were sterilized by overnight ultraviolet radiation (UV) to disinfect samples by destroying nucleic acids of microorganisms and harming their DNA, causing inactivation of cellular functions of organisms [56].

## 1.8 Characterization of samples

### 1.8.1 Scanning Electron Microscopy

Scanning Electron Microscopy images were taken with Hitachi S4700. The image belonging to a  $6 \times 4 \text{ mm}^2$  foam sample is shown in Fig. 1.12.

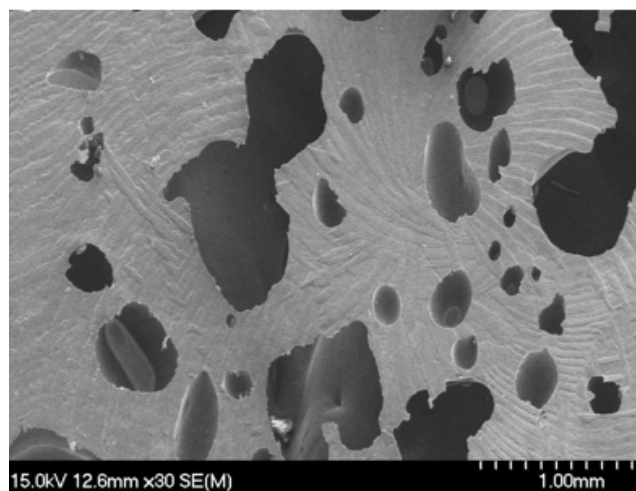


Figure 1.12 SEM image of foam ATSP sample

The image is belonging to a  $3 \times 3 \times 3 \text{ mm}^3$  bulk sample is shown in Fig. 1.13.

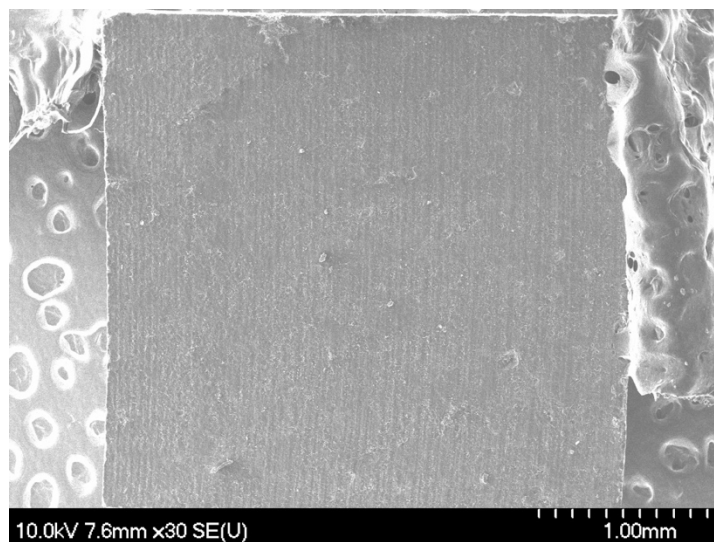


Figure 1.13 SEM image of bulk ATSP sample

The image belonging to a 5x5x5 mm<sup>3</sup> film sample is shown in Fig. 1.14.

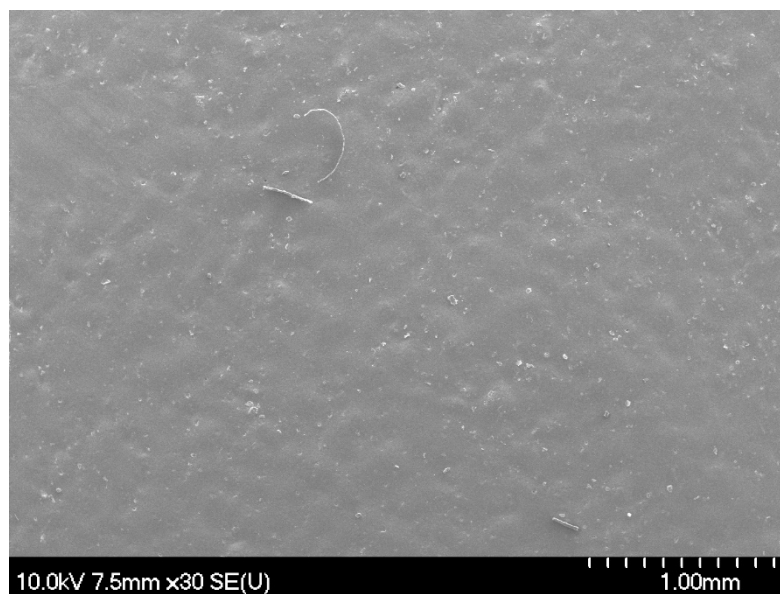


Figure 1.14 SEM image of film ATSP sample

### 1.8.2 Micro Computed Tomography

Foam specimens prepared for micro-computed tomography (Micro-Ct) were 6 mm in diameter and 4 mm in height (Fig 1.15). The Micro-Ct scans of the porous samples were done by utilizing an Xradia MicroXCT-200 which allowed to image the internal structure of the specimens. After centering the test specimens on the stage of the instrument, scans of the samples were taken with a 2 seconds exposure time. The obtained 721 images were processed with Xradia MicroXCT Reconstructor software and the final images were seen by XM3DViewer (Fig 1.16).



Figure 1.15 Foam Micro-Ct ATSP sample

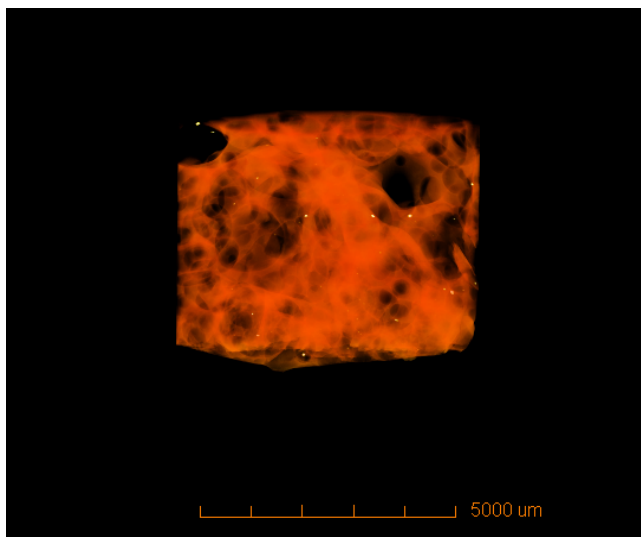


Figure 1.16 Micro-Ct Image of Foam ATSP sample

#### 1.8.2.1 Porosity Calculations of Foam Samples

Micro-Ct images were also utilized to measure the porosity of the foam samples. The average porosity value was calculated using five porous ATSP samples. For this calculation, intermode threshold method which changes the cross section to binary was applied to the images, and then solid area fraction was subtracted from each image. This subtraction equals the solid volume fraction which defines the porosity of samples. The black areas represent the pores while the white areas symbolize the bulk material (Fig 1.17) [57]. The porosity average of the five samples was 70% with 3.4 standard deviation.

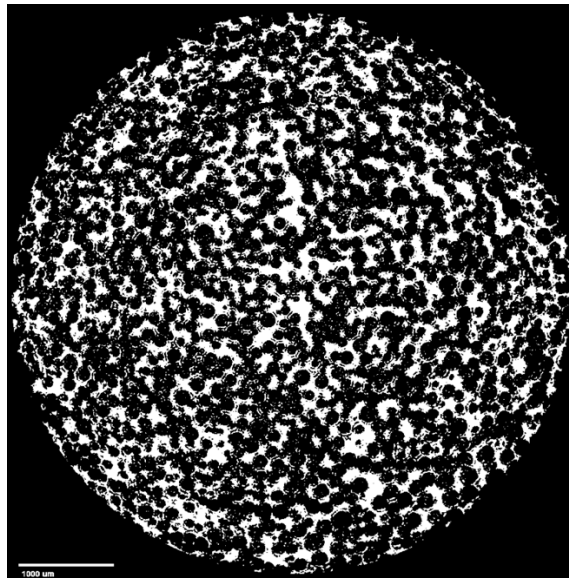


Figure 1.17 Example of Micro-Ct Image used in Porosity Calculation

#### 1.9 Statistical Analysis

One-way analysis of variance (ANOVA) was performed on metabolic activity. Significance was set at  $p > 0.05$ . Analysis of metabolic activity included  $n = 3$  samples per



group. The standard errors of the means were reported in the figures. There was no significant difference between groups and the results were consistent with each other.

## 1.10 Methods

### 1.10.1 Cell Culture Method Protocols

The human osteoblast cell line (hFOB 1.19 (ATCC® CRL-11372™) was cultured in the Type 1 medium. The proportion of 1:1 blend of Ham's F12 Medium Dulbecco's Modified Eagle's Medium with 2.5 millimolar (mM) L-glutamine (without phenol red) was the base medium for this cell line. For complete media, the accompanying parts: 0.3 Milligrams(mg) /milliliters (mL) G418 and fetal bovine serum as 10% of final concentration were added to the base medium.

The human osteoblasts' cell line hFOB 1.19 (ATCC® CRL-11372™) was obtained from the American Type Culture Collection (ATCC® CRL-11372™) and used as a cell line to analyze the cytotoxicity of ATSP in this research. This cell line was gained by transfection of limb tissue acquired from an improvised miscarriage. For these analyses, the cells were developed in 75 cm<sup>2</sup> cell culture (T-75) and placed in an incubator with 5 % CO<sub>2</sub> at 37 °C. The cell culture medium was changed every two days to refresh nutrients and maintain the correct pH levels, and cells were analyzed every day under optical microscopy to assess changes in morphology or their attachment.

### 1.10.2 The Protocol of Thawing, Culturing and Freezing Cell Line

For cell thawing, the medium was warmed in a water bath at 37 °C to defrost the cells in the cryogenic vial. When the substance was dissolved, the cell suspension was moved into a 15mL rotator tube, and the appropriate amount of culture medium was added and afterward centrifuged. The suspension obtained after centrifugation was expelled, and cells were

resuspended into a 25 cm<sup>2</sup> cell culture flasks with 4mL culture media, and the flask was placed in the incubator.

When the cells reached 80 % confluency after the incubation of the cell culture flasks, the subculturing of cells was required. The subculture of the cell lines was done by discarding the medium and washing the cells with 2-4mL Dulbecco's phosphate-buffered saline (DPBS) and then incubating them with a 2-4mL trypsin-ethylene diamine tetra acetic corrosive (trypsin-EDTA) for 5 to 15 minutes at 37 °C. In the incubator, cells detached from the surface. The appropriate cell culture medium (either human skeletal muscle cell culture medium or human osteoblast cell culture medium) was added to neutralize the activity of the catalyst (trypsin). Cells were centrifuged in a 50mL tube for 3 minutes at 1000 rpm (150 x g) and resuspended into new cell culture flasks with 12mL culture media in a part proportion of 1:4.

After resuspension, some number of cells were frozen in liquid nitrogen at below – 130 °C to keep cells in stock and use them for further studies. The cells were detached by trypsinization (as portrayed above) and re-suspended in cryogenic vials with solidifying blend which includes FBS containing 10 % (volume/volume) dimethyl sulfoxide (DMSO) as a cryoprotective operator.

#### 1.10.3 Protocol of MTT Assays

5 mg MTT powder was added into 1mL autoclaved water to prepare the MTT reagent which was kept at 2 - 8° C in the dark. Since 1mL of solution and around 400,000 cells are required for 12 well plates, while 0.5mL solution and 200,000 cells at confluency are used for 24 well plates use, six-well plates were used with the cell number 400,000 in each well [58]. Each condition was done in triplicate. Firstly, the flasks were trypsinized and the appropriate culture media, which is the double amount of trypsin (either human skeletal muscle cell media or human

osteoblast cell media according to the cell line used in the analysis), were added to trypsinized cells to neutralize the effect of trypsin. After that, the suspension which included trypsinized cells with neutralization media was centrifuged using a sterile centrifugation tube at 1000 rpm (150 x g) for 3 minutes. Then, the media was removed and cells were resuspended with the appropriate media. The cells were then counted, and 400,000 cells were added into each six-well plate. Lastly, the plate was placed into an incubator overnight. 24 hours later, the media was removed and new media was added after washing with DPBS. Then, the cells were treated with neat and composite bulk, film and foam ATSP samples with the final volume 4mL. 44 hours later, 200  $\mu$ L of 5 mg/mL MTT solution was added to each well including control wells which consisted of only the MTT solution but no material. Incubation of the well for 4 hours at 37 °C in culture hood was the next step of this process. After the incubation period, the media was removed carefully and 200  $\mu$ L MTT solvent was added, and the absorbance at 570 nm was obtained after shaking for 1 minute (Fig. 1.18).

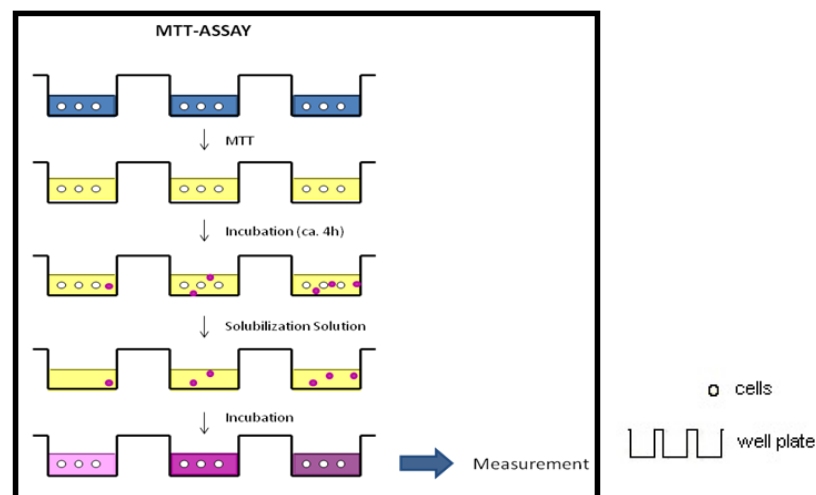


Figure 1.18 The steps of the MTT assay

#### 1.10.4 Method Setup

The MTT samples and test controls were arranged in three replicates on four 6-well plates, according to the layout shown in Fig. 1.19.

In the test 400,000 cells for each well were put in 4mL culture medium with the samples. The cells were first seeded and the materials were placed inside the well thereafter. Cells were watched day by day. The cytotoxicity test of ATSP samples were mainly categorized into two different groups: neat ATSP and Composite ATSP (ATSP+HA) and these two group had sub-groups as bulk, film, and foam. These sub groups were tripled and done with 3 different concentrations of material (8mg/mL; 16mg/mL; 24 mg/mL) and were evaluated by the same number (400,000 cells) of osteoblasts cells (hFOB1.19). Cell viability was surveyed after 48, hours and assessed as portrayed in section 3.5.3.

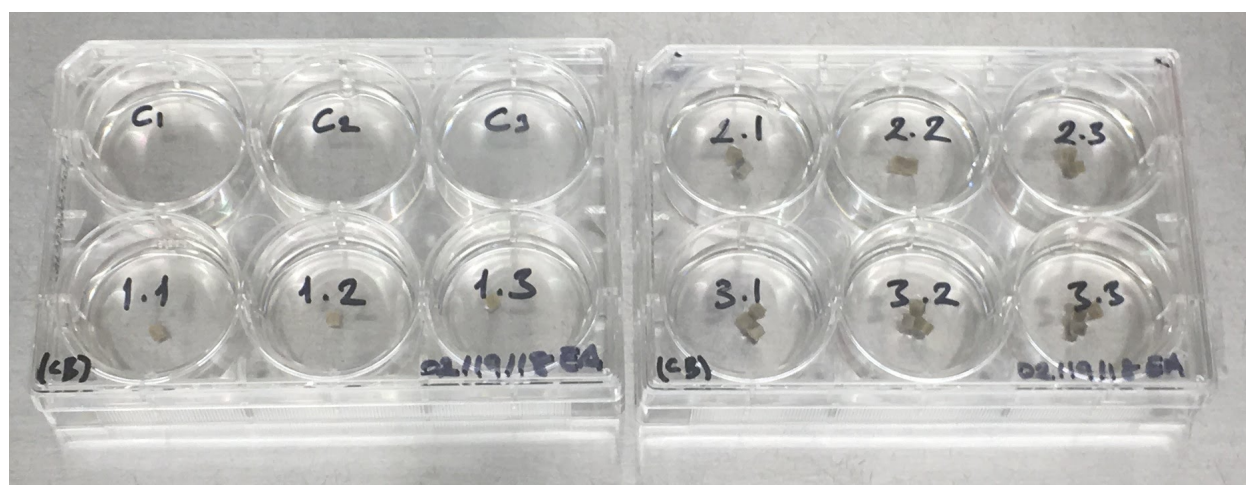


Figure1.19 Arrangements of the material samples inside the 6-well plate

#### 1.10.5 Calculations and Evaluation of Obtained Absorbance Values

The absorbance readings from each well were put in the equation below to calculate the cell survival rate since MTT solvent reduction is accepted as proportional to the cell metabolic

activity. The absorbance readings were obtained by the reduction MTT solvent (yellow color solvent) to a dark purple insoluble formazan processed by the chemical succinate dehydrogenase in the mitochondria of metabolically active cells (Fig. 1.20).

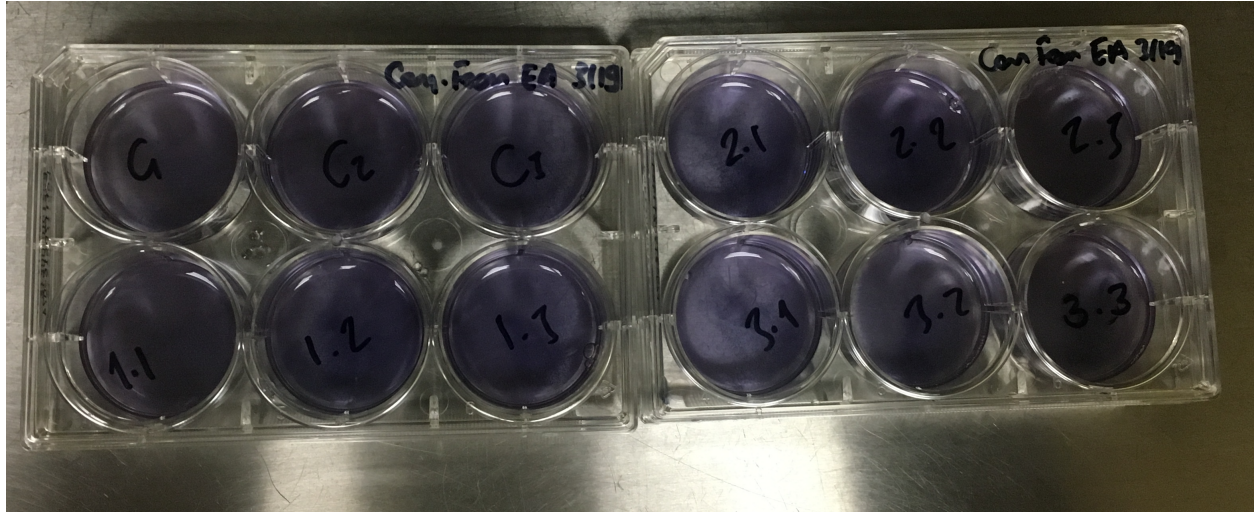


Figure1.20 The reduction of MTT to formazon

Calculation of the cell survival rate;

$$MTT = \left( \frac{A_{\lambda}}{A_{\lambda control}} \right) * 100 \quad [\text{Equation 1}]$$

$A_{MTT}$  = Absorbance value of released MTT

$A$  = Absorbance of test well

$\lambda = 5700\text{nm}$

### 1.11 Results and Discussion

The biocompatibility of neat and composite ATSP samples in the form of bulk, film, and foam were analyzed in-vitro by measuring mitochondrial dehydrogenase activity (MTT test) for 48 hours and by the analysis of cell viability of human osteoblasts cells cultured in indirect contact with 3 different neat and composite ATSP forms. Also, three different concentrations 8 mg/mL, 16 mg/mL, and 24 mg/mL for each form were tested. These concentrations were

obtained from changing the weight of the neat and composite ATSP samples (doubling and tripling the weight of ATSP) and keeping the number of cells the same to examine the effect of increasing concentration on human osteoblast cells. The effect of HA on the cell viability was analyzed by the composite materials. Experiments were done in a cell culture laboratory according to the requirements of ISO 10993 (biological evaluation of medical devices standard) to determine the cytotoxicity of the medical devices by quantitative methods (MTT). The results were obtained from MTT absorption and reflected mitochondrial activity in the viable cells. The percentage of cell viability higher than 90% was accepted as a good biocompatibility for the tested ATSP samples in different concentrations. The absorption for control cells was accepted as 100% viability. The rate of cytotoxicity was relied on the cell viability proportional to the control group. It was accepted that greater than 85% is non-cytotoxic, 60%– 85% is slightly cytotoxic, 30%– 59% is moderately cytotoxic, and less than 30% severely cytotoxic.

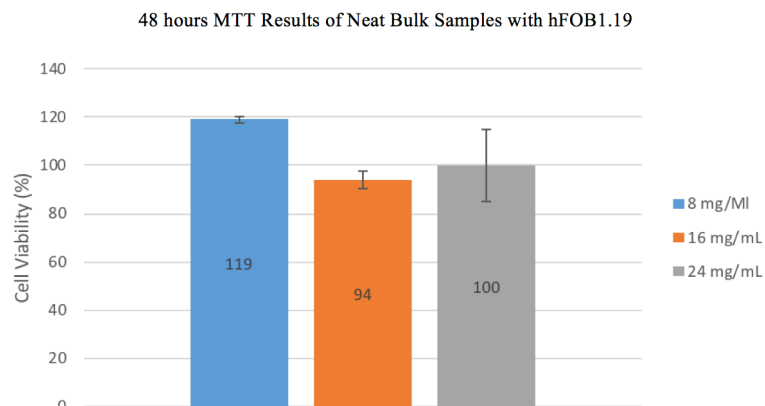


Figure 1.21 Cell viability results of neat bulk samples by MTT

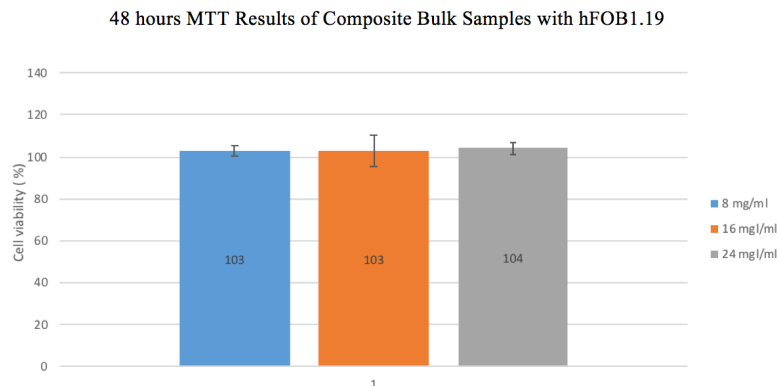


Figure 1.22 Cell viability results of composite bulk samples by MTT

In the metabolic cell activity results of neat and composite bulk samples with the MTT test by human osteoblast cells (Fig. 1.21 and Fig. 1.22), it is noticeable that neat and composite bulk ATSP samples did not demonstrate any toxicity for all concentration and all the values are higher than 90%. Furthermore, increase in the concentration did not change the results for all bulk samples ( $p>0.05$ ). Composite bulk samples made of the mixture of HA and ATSP oligomers were used to investigate the HA effect over enhancing the metabolic cell activity. However, there was no increase in the cell activity with the presence of the HA (Fig. 1.22), and the results were similar to the neat bulk material ( $p>0.05$ ). Also, the result belonged to 8 mg/mL neat bulk sample was higher than 100%. When the results are over 100%, this could be a pipetting issue since the accuracy and precision of pipetting cells with the same density are important criteria in cytotoxicity assays. For each time, it is important to seed the same number of cells into the wells because seeding different cell density affects the results. When more cells pipet to a well, we can get a higher metabolic activity than others and sometimes the cell viability will be over 100%. To avoid inaccuracies in the results, the different steps of the plating cell should be considered such as pipetting the cells at vertical angle, gently mixing of the solution before pipetting, and using low immersion depth. Also, cells are experiencing shear

force during pipetting, and this force will negatively affect viable cells. Hence pipetting slowly and gently is another requirement.

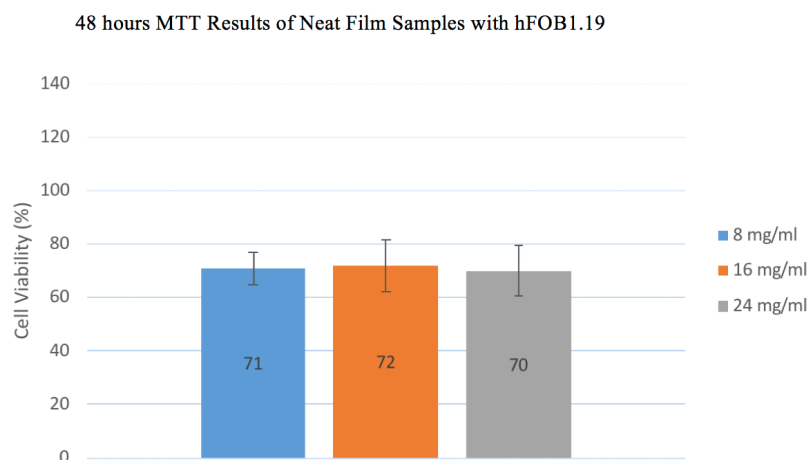


Figure 1.23 Cell viability results of neat film samples by MTT

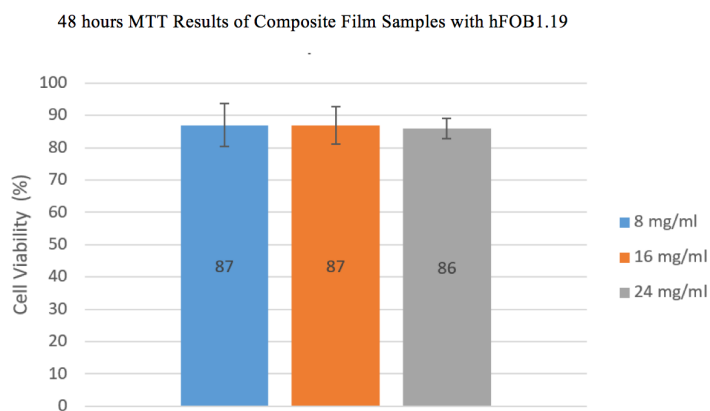


Figure 1.24 Cell viability results of composite film samples by MTT

The lowest cell viability results, as compared to the control group, belonged to neat film samples, around 70% for each concentration (Fig. 1.23). Composite film results were around 90%; these results had a satisfactory level of biocompatibility (Fig. 1.24). The low metabolic activity results for neat film could be due to either their adherence to the bottom of well plate or



tedious handling process. During the discarding process of the film samples, the cells could have been harmed because the cells were growing at bottom of the culture flasks. While taking the film samples out, it was possible to harm them with a physical stimulus. On the other side, all the results for neat and composite film are consistent with each other. Both the increase in the concentration and the presence of HA did not change the results ( $p>0.05$ ).

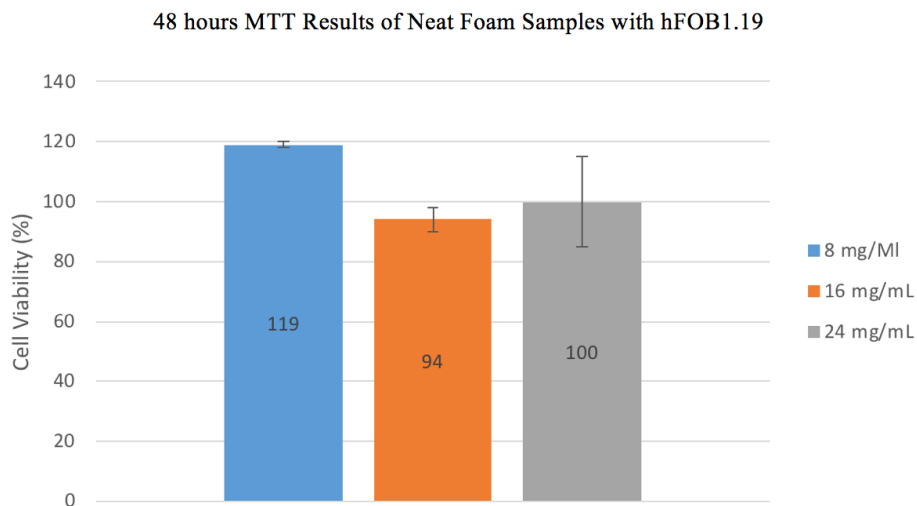


Figure 1.25 Cell viability results of neat foam samples by MTT

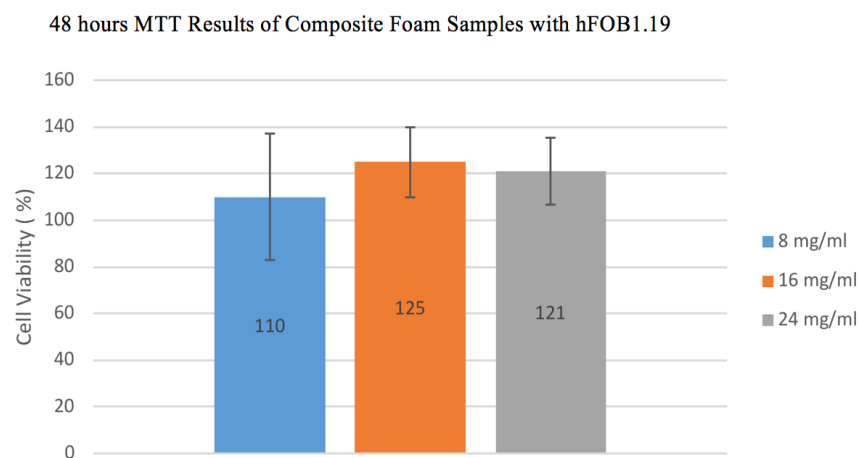


Figure 1.26 Cell viability results of composite foam samples by MTT

The neat and composite foam samples possessed the highest cell activity (Fig. 1.25 and Fig. 1.26). The results of foam samples were around or higher than 100%. The absorbance readings are based on the concentration of MTT, incubation time, the number of viable cells, and the metabolic activity of these cells. Even though the concentration of the MTT, incubation time, and the number of the viable cells were the same with others, there could be some abnormality in these criteria such as more cells than control group could be seeded in those wells. On the other hand, the structure and pore size of the ATSP could positively affect the results; also, the compound of the ATSP could be the reason for the high level of cellular activity. The presence of HA and different concentration treatment did not significantly affect the results, and the results were consistent with each other ( $p>0.05$ ).

It was mentioned in the Introduction that new biomaterials may show an adverse effect to the body, and thus they should be subjected to particular toxicity assays before their utilization in the body. In-vitro assays have been used to successfully to investigate the biocompatibility of a new material. The cytotoxicity assays are accepted as fundamental in-vitro assays to determine the potential toxicity of a new biomaterial. In-vitro assays for assessing the biocompatibility are able to distinguish the toxic material. They also provide the rapid estimation, standardized guidelines, and comparable data [59]. In this study, the biocompatibility of three different forms (bulk, film, and foam) of neat and composite ATSP were tested with the indirect contact test by MTT assay which analyzed extracts from each sample. These results showed that all of the analyzed samples except the neat film samples, did not show a cytotoxic effect and did not block cell proliferation, and thus have an acceptable level of biocompatibility. Also, the MTT assay revealed that none of the extracts from the tested samples affected the viability of the cells. However, as compared to the control group, the cell viability was around 70% for each

concentration of a neat film. Therefore, the neat film samples could be accepted as slightly cytotoxic. The reason for the low metabolic activity of neat films would be the higher surface area of film samples or the adherence of film samples to the bottom of the well plate that may have harmed the cells. Also, there were some results which have more than 100% cell viability. There is a possibility that the cells may have increased enzymatic activity without developing an effect on cell number or cell viability. Also, if the substance demonstrates no toxicity at a certain concentration, the viability can surpass 100%. There is another possibility that more cells than control group could be seeded in those wells due to small pipetting errors. However, if the metabolic activity percentage was far beyond 100%, it could mean the substance might also have an influence on the cells [60]. Furthermore, ATSP alone or in combination with other materials have a potential to be used in medical applications due to their inertness, tribological properties, high wear resistance, and excellent mechanical properties. Even though synthetic polymers do not have a functional group for stimulation of cell adhesion, they can bind bioactive particles like hydroxyapatite (HA) or protein sequences, which activate cell reactions [61]. HA was preferred as a filler in this experiment because HA has a similar chemical composition as the mineral component of bone, and it is well-known for its biocompatibility and osteoconductivity. Also, it is shown that HA-reinforced polymer composites increase biological properties [62]. However, the results showed that there is no positive effect of HA on the cell viability, the composite sample results were similar to neat results for each structure.

### 1.12 Future Works

Even though the neat and composite ATSP are promising candidates for therapeutic applications, the potential of ATSP for medical application has not been yet fully explored. Therefore, more in-vitro assays with different cell lines should be done in order to compare and

determine if the results are consistent with each other. Currently, the MTT cytotoxicity assays using human skeletal muscle cells are being conducted for neat and composite film, bulk and foam ATSP samples. Also, the long-term effectiveness of ATSP must be analyzed. In-vitro assays are the initial verifications of the in-vivo results, but the in-vitro results can cause misleading results while in-vivo studies provide conclusive results about new materials. Therefore, in-vivo studies are recommended for ATSP.

## CHAPTER 2: HUMAN MESENCHYMAL STEM CELLS DIFFERENTIATION REGULATED BY NEAT ATSP AND COMPOSITE ATSP (%10 HYDROXYAPATITE CONTENT WITHIN ATSP)

### 2.1 Introduction

Stem cells are particular cell types which can reestablish themselves through cell division and differentiate into multi-lineage cells. These cells are defined as embryonic cells (ESCs), induced pluripotent cells (iPSCs), and adult stem cells. Mesenchymal stem cells (MSCs) are a type of adult stem cells which can be obtained from human and animal sources. Human MSCs (hMSCs) are the non-hematopoietic, multipotent stem cells with the ability to differentiate into osteocytes, adipocytes, and chondrocytes [63].

Additionally, stem cells play a fundamental role in tissue regeneration in-vivo through lineage differentiation caused by environmental components. Previously, biochemical signs were the main point of induced stem cell differentiation. As revealed by Engler et al. 2006 [64], stem cells differentiation is intervened by biophysical signals, which could likewise perform as a critical inducer. Hence, producing dynamic biophysical signals to coordinate stem cell fate through uniquely composed material microstructures has become important. These outlined biophysical signals incorporate the material elasticity/rigidity characteristics, micro patterned structure, and porous structure. Many examinations have been done on material coordinated mesenchymal, embryonic, adipose stem cell, and differentiation [65].

Recent studies have indicated that substrate signals significantly influence the growth and differentiation of mesenchymal stem cells (MSCs), and that in-vitro and in-vivo differentiation of MSCs along the osteogenic pathway appears to be highly dependent on the substrate composition. For the use of hMSCs in bone regeneration, it is particularly important to

understand the interactions between hMSCs and materials because cell–material interactions play an essential role in the bonding of implant materials to native bone tissue. [66]

Natural materials demonstrate excellent potential as an implant material as a result of their convenience and innate biocompatibility, while synthetic materials have an advantage that they can be engineered to have different properties. A few cases of engineered materials are polylactic corrosive (PLA), polycaprolactone (PCL), and poly(lactide-co-glycolide) (PLGA) and  $\beta$  tricalcium phosphate ( $\beta$  TCP) [67].

Mesenchymal stem cells (MSCs) are the most broadly studied cell lines in biomedical applications. These cells differentiate along the osteogenic lineage when seeded on various substrates including hydroxyapatite containing frameworks and can be utilized as a remedial choice to recover different tissues [66]. Hydroxyapatite (HA) has conclusively affirmed its osteoinductive properties in-vitro and in-vivo [68].

Since the cell viability assays with MTT by human osteoblast cell line showed that the ATSP forms did not have a significant cytotoxic effect (Chapter 1) and the foam had the highest cellular activity results, the direct contact interaction between hMSCs and the ATSP foam directly was investigated in this chapter. Our goal was to characterize the response of human mesenchymal stem cells (hMSCs) to a novel porous neat and composite materials for bone tissue engineering applications. The morphology of the porous neat ATSP and composite was investigated by scanning electron microscopy (SEM). The hMSCs cell proliferation and differentiation into the osteoblastic phenotype was evaluated using alamarBlue® assay and RT-PCR.

## 2.2. Materials

### 2.2.1 Foam Samples

The foam structure is produced by self-generated blowing agent (acetic acid) caused by the endothermic condensation which was generated between aromatic based acetoxy and carboxylic acid oligomers. Two different type of foam samples including neat ATSP (scaffold) and ATSP with 10% HA (composite) were produced 6 mm in diameter and 4 mm in height with 70% porosity. Two different samples were tested in both regular growth media and osteogenic media. The design of the assay was categorized as scaffolds with growth media, scaffold with osteogenic media, composite with osteogenic media, and composite with growth media.

### 2.3. Cell Culture, Assay, and Imaging Protocols

In this chapter, the human mesenchymal cell line (hMSCs) (Lonza PT-2501) was used. These cells lines were disconnected from ordinary (non-diabetic) adult human bone marrow pulled back from bilateral punctures of the posterior iliac crests of typical volunteers. Cells were cultured in two different media (complete growth media and osteogenic media) and put in a humidified atmosphere containing 5% CO<sub>2</sub> at 37°C. The new media was added twice per week to maintain the pH of the environment and adequate nutrients for cells. The passage five cell lines were used for all experiments.

#### 2.3.1. hMSC culture and differentiation protocol

Both protocols, normal growth media and osteogenic media, were performed in the laminar flow hood [69]. The reagents of the completed normal growth media for the human mesenchymal cell line (hMSCs) were 445mL low glucose DMEM (Fisher SH30022.FS), 50mL MSC-validated fetal bovine serum (Invitrogen 12662-029), and 5mL antibiotic-antimycotic

(Invitrogen 15140-122). The osteogenic media was also prepared in the same way with the normal growth media protocol but additionally 0.1 micro molar ( $\mu\text{M}$ ) dexamethasone (Sigma D4902-100MG); 10 mM beta-glycerophosphate (Sigma G9422-10G); 50 micro molar ( $\mu\text{M}$ ) ascorbic acid (Sigma A4403-100MG) were added. After the completion of both media, sterilization was done by a filter before use [69].

### 2.3.2. MSC thawing and counting procedure

Before thawing a frozen cell vial, the complete MSC medium was placed in a water bath and warmed to 37°C. The frozen cell vials were put in water bath for 2 minutes in 37°C. Then, the thawed cells and freezing medium were transferred to a 15mL centrifuge tube. The complete MSC medium was added, and the volume was brought up to 9mL. The 10mL cell suspension was removed for counting. The 15mL centrifugation tube was placed in the centrifuge at 600 g for five minutes. After the cells were spun, they were seeded at the required density (usually 5,000-6,000 cells/cm<sup>2</sup>). The media was used according to the flasks' size; around 10-12 mL for a 100-mm dish, 12-14 mL for a T75, or 7-8 mL for a T25. The flask(s) were placed into the incubator. The confluence was checked every 24 h, and the media of cells were changed twice a week [69].

While cells were spinning down, the 10  $\mu\text{L}$  cell suspension for counting were mixed with 10mL of Trypan blue, and the mixture was pipetted several times to mix the stain and cell suspension. Then, 10mL of the stain/cell suspension was pipetted into the hemocytometer to count the number of alive cells. The average number of cells per area was utilized to measure the cell population. For this count, the dilation element was accepted as 2 (1:1 ratio of cell suspension to Trypan blue) [69].



$$TCP = (MCR) * D * 10,000 * (CSV)$$

Equation 2 [69]

TCP = Total Cell Population

MCR = Mean Cells per Region

D = Dilution

CSV = Cell Suspension Volume

### 2.3.3. MSC passaging procedure

The complete MSC media, sterile PBS, and 3mL trypsin-EDTA were warmed in a water bath to 37°C. All of the media from each T75 flask were removed, and 10mL of PBS was added to per T75 waited for 30 seconds. The PBS was removed and 3mL of trypsin was added per T75 flask. Then, the flasks were returned to the incubator for 8 minutes to allow for the cells to detach from the flasks. 6mL of complete MSC media was added to each flask to neutralize the trypsin. The suspension, made up of the trypsin, additional media, and cells, was put into a conical tube. The 10mL cell suspension was removed for counting. Then, a tapered tube was centrifuged at 600 g for 5 minutes. The media supernatant was aspirated, and new media was added to dilute cells to the desired concentration. The cells were seeded according to the requirement [69]. The cell counting was done as explained under the MSC thawing and counting procedure section.

### 2.3.4. MSC freezing procedure

For MSC freezing procedure, the MSC passaging procedure was followed until aspirating the media and resuspending. After this, the volume of freezing media that is required to resuspend  $1-10 \times 10^6$  cells per mL was added to cryopreservation vial. The reagents of the

freezing media were 50% complete MSC media, 40% FBS, 10% DMSO. 1mL cryogenic tubes were filled with cells and freezing media in the ratio of 1:1. Cryogenic tubes were placed in a -80°C freezer [69].

#### 2.4. Quantification of MSC metabolic activity

hMSCs cells were cultured until they reached 80% confluency before preparing the plates for the cytotoxicity assay. Cells were seeded on the dry scaffold at a density of  $7.7 \times 10^4$  cells per well in 24-well-plates (Fig. 2.1). Every row of the plates was treated with normal growth and osteogenic media, and the experiments were performed in triplicate. The readings of the cell viability using the alamarBlue® assay were performed for one day, four days, and seven days.

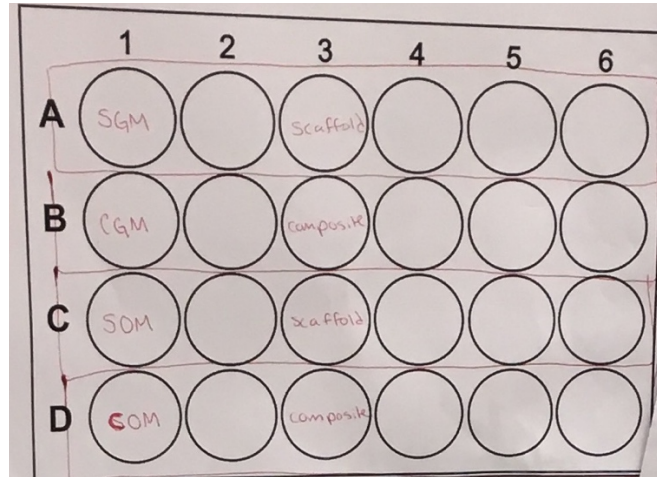


Figure 2.1. The schematic of alamarBlue® Plate

The metabolic activity of MSCs in scaffolds and composites were assessed using the alamarBlue® assay (Invitrogen). AlamarBlue® quantifies the mitochondrial metabolic activity by the continuous reduction of the alamarBlue® dye (resazurin) to the fluorescent byproduct resorufin by healthy, active cells. Fluorescence was measured (excitation: 540 nm, emission: 600 nm) on a fluorescent spectrophotometer [69].

#### 2.4.1. Ethylene Oxide Sterilization of Scaffold

The foam samples were sterilized by exposure of the sample to the ethylene oxide, which is a sterilization method of a medical device or component.

The EO high reactivity, as communicated by the high energy of its exergonic ignition response, in combination with its high diffusivity, is of real significance for the inactivation of microorganisms. The consequence of its effective alkylation response with cell constituents of organisms are thought that there is no need for metabolic activation, and its inactivation properties are, for example, nucleic acid and proteins, including compounds, which result in denaturation [70].

The EO sterilization method was actualized according to ANSI/AAMI/ISO 10993-7: 2008, which defines acceptable limits for residual ethylene oxide (EO) in an individual EO-sterilized medical device. The lethality of EO sterilization relies upon the accompanying four process parameters: (i) the concentration of EO, (ii) exposure time, (iii) temperature, and (iv) humidity. The concentration of EO for sterilization was 100% EO at low temperature (30–60°C). As described in the protocol, the samples were placed into gas-penetrable packs and put in the sterilizer for three hours. Overnight air circulation in the encompassing environment was then performed [70].

#### 2.4.2. Scaffold hydration

All plates were labeled according to the combinations of different samples and different media as shown. A total of 72 samples were used, and they were placed into six-well plates as each well had six scaffolds. The samples were set according to the type, and 4mL of appropriate media were added to each well. Then, the plate was placed in the incubator for 24 hours (Fig 2.2).



Figure 2.2 from left to right; composite (ATSP+HA) with osteogenic growth media (COM), composite (ATSP+HA) with regular growth media (CGM), scaffold (neat ATSP) with osteogenic media (SOM), scaffold (neat ATSP) with regular growth media (SGM)

#### 2.4.3. Standard curve for alamarBlue®

Before beginning the assay, a standard curve was created with a known number of cells. The standard had eight sample points. These points included a well with just media, a well with media and alamarBlue®, and 24 wells with media, alamarBlue®, and an alternate number of cells. An illustration standard setup was as shown in Fig 2.3:

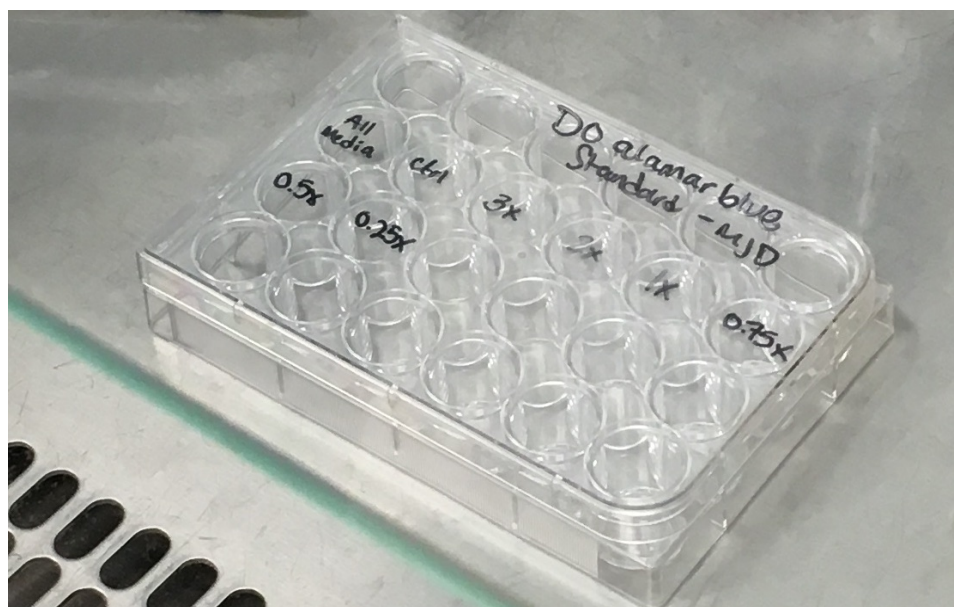


Figure 2.3 Day 0- alamarBlue® standard curve plate

The well containing all media was a negative control while the background control was obtained from a control-well, and other wells were utilized to make the standard curve. The diluted cell number calculations were calculated as below:

Table 2.1. The calculations of alamarBlue® standard curve

<u>alamarBlue®</u> standard curve			
Total cells needed:	$(3*\text{cells})+(2*\text{cells})+(\text{cells})+(0.75*\text{cells})+(0.5*\text{cells})+(0.25*\text{cells})$		
	AB	cells (μL)	media
control 1	0	0	1mL
control 2	100	0	900
0.25x	100	10	890
0.5x	100	20	880
0.75x	100	30	870
1x	100	40	860
2x	100	80	820

The standard curve plate was placed on the shaker (~50 rpm) in the incubated at 37°C for 4 hours. During this process, the viable cells changed inflorescent resazurin to the fluorescent resorufin. After this process, a curve of known cell number and absorbance was obtained, and the curve was used to calculate the number of cells from absorbance readings for other days.

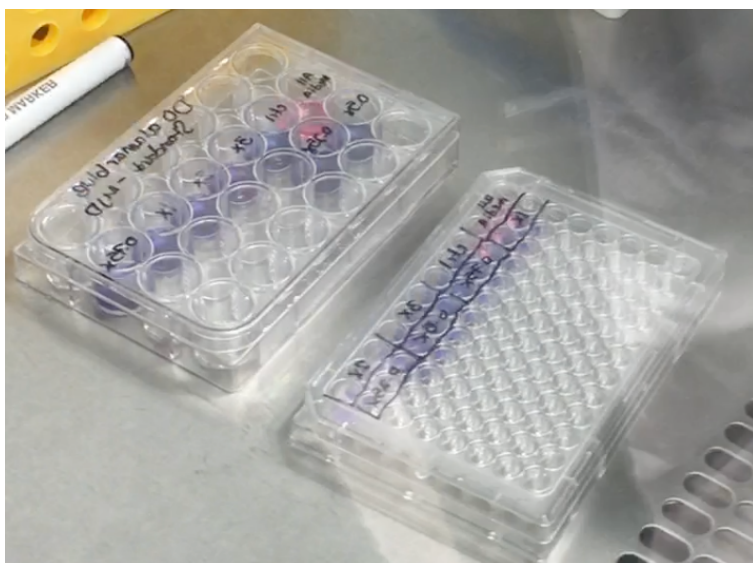


Figure 2.4 The alamarBlue® reduction into standard plate

After incubation, 100  $\mu$ L were taken from each example and placed into a 96-well plate to make three replications. The fluorescence (excitation: 540 nm, reference: 600 nm) on the spectrophotometer were measured by using 'AlamarBlue® F200' program. The average of each data points was calculated to draw the standard curve; the change of the fluorescence reading was calculated by subtracting the results from well 2 (control well) as shown the formula below. The standard bend is made by plotting cell number as a component of equal fluorescent force (Fig 2.4).

Table 2.2. The calculations of percentage reduction of alamarBlue®

Percentage reduction of alamar blue:		$\frac{(O2 \cdot A1) - (O1 \cdot A2)}{(R1 \cdot N2) - (R2 \cdot N1)}$	x100
O1=	molar extinction coefficient E of oxidized alamar blue at 570nm		
O2=	E of oxidized alamar blue at 600nm		
R1=	E of reduced alamar blue (red) at 570nm		
R2=	E of reduced alamard blue at 600nm		
A1=	absorbance of test wells at 570nm		
A2=	absorbance of test wells at 600nm		
N1=	absorbance of negative control well (media plus alamar blue but no cells) at 570nm		
N2=	absorbance of negative control well (media plus alamar blue but no cells) at 600nm		
	<b>Wavelength</b>	<b>Reduced R</b>	<b>Oxidized O</b>
	540nm	104395	47619
	570nm	155677	80586
	600nm	14652	117216
	630nm	5494	34798

#### 2.4.4. Seeding cell on the scaffold

Six samples with 6 mm in diameter and four (4) mm in thickness for each group were used. 20µl total cells (so 10µl each side) were seeded on the scaffold and then we waited 30 minutes on each side (hour in total) before adding 1mL of media. The samples were placed according to their group; (i) scaffold (neat ATSP) with growth media, (ii) scaffold with osteogenic media, (iii) composite (ATSP+HA) with growth media, and (iv) composite with osteogenic media were put into wells of 24-well tissue culture plate. Then, the samples were placed into the incubator at 37°C and 5% CO<sub>2</sub>.

#### 2.4.5. alamarBlue® Protocol

At each chosen time point after seeding the cells (i.e., 24, 96, and 168 hours) the samples were taken out of the incubator, washed in PBS, and then placed each in a 24 well plate with 100 µl alamarBlue® and 900µl media, with one of the wells being a control again. The plate was put in the incubator on a shaker for the same period as the standard plate, and then the foam materials were removed and placed them in their original wells. A short time later 50 µL were

taken from each well and suspended into a 96-well plate in triplicate and we read the absorbance of the plate. The absorbance was estimated spectrophotometrically at 570 nm and 600 nm. We then used the same protocols on day 4 and day 7, doing the same procedure [69].

## 2.5. RT PCR

The qualitative assays are the most widely recognized protocols for analyzing in-vitro osteogenesis. These assays are dependent on dyeing insoluble parts of the discharged ECM, such as calcium, phosphate, and collagen. In addition to this technique, the colorimetric process of labeling molecules (reporter) by alkaline phosphatases (ALP) was utilized to investigate osteogenesis. These tests had restrictions in that they depended vigorously on microscopic visualization of the dying and objectivity of the specialist. Therefore, quantitative RT-PCR and microarray examinations are preferred assays among others for estimating osteogenesis, because these techniques are delicate and more quantifiable [71].

Real-time PCR (or qPCR) is a broadly utilized gold standard for quantitative investigation of gene expression. The recognition of intensification of DNA in real time as PCR is detected by the utilization of fluorescent reporter, which is the crucial component of the PCR. The fluorescent reporter signal intensity is relative to the number of amplified DNA molecules. Between 2001 and 2010, RT-PCR has been utilized as a ground-breaking assay for genotyping (Alker, 2004) [72], measuring viral load, and gene copy number tests. RT-PCR is the highest quality level of gene expression level test [71].

There are two ascertainment strategies for RT-PCR. The first strategy, which is called the TaqMan test, depends on a particular probe sequence. The TaqMan analysis is a generally utilized RT-PCR assay because of its affectability and specificity. DNA polymerase 5'– 3' exonuclease activity form the basis of the TaqMan assay. Figure 2.5 shows the schematic of



TaqMan test protocol. The TaqMan test is a sequence-specific oligonucleotide with a correspondent fluorescent color at 5' end and a quencher color at 3' end. When there is no probe hydrolysis by TaqMan DNA polymerase process, a quencher fluorescent stain will absorb the reporter stain's emitted fluorescent light. However, when Taq DNA polymerase hydrolyzes the probe, the 5' reporter fluorescence stain is isolated from quencher stain. Hence, the quenching effect will be lost and the discharged 5' reporter fluorescent stain signal can be measured by the RT-PCR instrument [72].

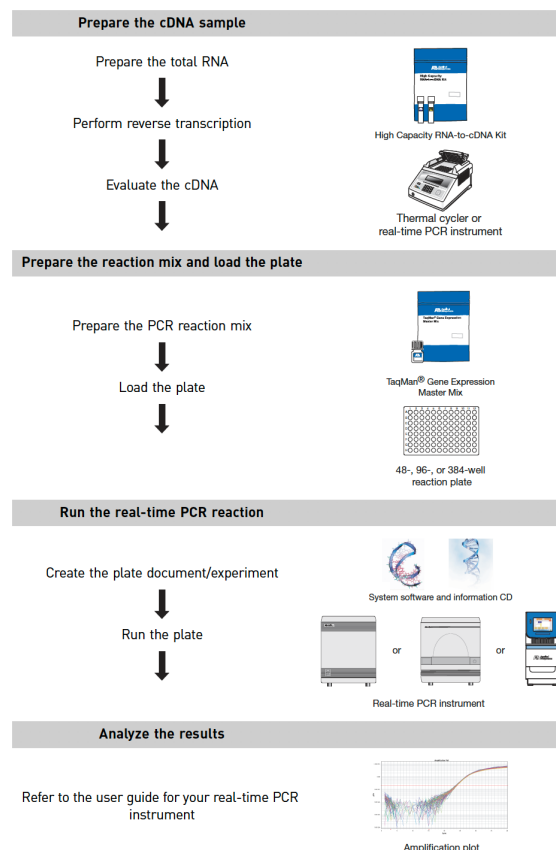


Figure 2.5 The schematic of TaqMan test protocol [72]

### 2.5.1 RT PCR Procedure

The extraction and quantification of total RNA is the first step to obtain the appropriate amount of RNA, which is used to implement first-strand cDNA synthesis through reverse transcription. Typically, greater than 10 ng of cDNA is preferred per well for real-time RT-PCR experiment.

RNA was extracted from MSC-seeded platforms at time-frames one, four, and seven days, employing a RNeasy Plant Mini kit (Qiagen, Valencia, CA) [69] and transcribed to cDNA with the QuantiTect Reverse Transcription pack (Qiagen). PCR responses were performed in triplicate utilizing TaqMan on an Applied Biosystems 7900HT Fast Real-Time PCR framework. Since Mesenchymal Stem Cells (MSCs), which are viewed as crucial cell elements for the usage of cell-based ideas in the field of regenerative medication, have been effectively used to regenerate wounded bone, ligament, cardiovascular tissue, and other types of tissues. Specific transcription factors and signaling pathways manage the osteogenic differentiation of MSCs. The osteopontin (SPP1), bone sialoprotein 2 (IBSP), runt-related translation factor 2 (RUNX2), and GAPDH were used for gene expression in this research. Runt-related translation factor 2 (Runx-2) is accepted as an early osteogenic differentiation marker. Decrease in the expression of Runx-2 results in insufficient bone formation since this translation factor is viewed as a main controller of osteogenesis. Runx-2 influences other bone-particular genes, bone sialoprotein 2 (IBSP), by attaching to particular promoter districts. The expression of IBSP is mostly seen in mineralized tissue as it stimulates mineral formation in the bone. The high-level expression of IBSP means the mineral and nodule formation occurs in the material or increase in the osteoblast related gene expression are seen [73]. Runx-2 is known as a crucial factor for osteogenic differentiation and also it plays a fundamental role in formation of mineralized tissue. Osteopontin (SPP1) is used as an early osteogenic marker. SPP1 is a protein found in bone matrix, which regulates the

biomineralization. The presence of the SSP1 expression in the results suggests that this material can act as a structural substance [74]. Glyceraldehyde 3-phosphate dehydrogenase (GAPDH) was used as a housekeeping gene, which is one of the most commonly used housekeeping genes in comparisons of gene expression data. Data were examined by the Comparative CT Method ( $\Delta\Delta$  CT Method), which is used to evaluate a lot of samples results. The Comparative CT Method utilizes an arithmetic formula to accomplish the outcome for the relative quantitation [72].

#### Step 1-RNA isolation

The platform was washed out with PBS, and afterward, RNA was removed from scaffolds through an RNeasy Plant Mini (Qiagen 74904) kit, as beforehand depicted at Duffy, McFadden, et al. 2011 [75]. The RNA isolation protocol is explained as follows: 500  $\mu$ L of RLT lysis buffer supplemented with  $\beta$ -mercaptoethanol was added to each tube and was kept on ice for  $\sim$  5 min. The cells were shaken regularly to assist cushion to infiltrate through the scaffolds. The appropriate amount of lysis buffer was measured, and it was pipetted into a labeled QIAShredder column with the scaffold. The tubes were spun at 14,000 rpm for 2.5 minutes. 500  $\mu$ L of 70% ethanol was added to each sample [69].

Half of the lysate + ethanol solution was added to the labeled RNeasy column (with a 2mL collection tube), and it was spun at 12,000 rpm for 30 seconds. After that, the remaining liquid was discarded, and the column was replaced. The remaining lysate + ethanol solution was added to the column and centrifuged at 12,000 rpm for 30 seconds. Again, the obtained suspension was discarded, and the column was replaced. 700  $\mu$ L Buffer RW1 was added to the column which was centrifuged at 12,000 rpm for 30 seconds. The same procedures, discarding flow and returning the column processes, were repeated. After this, 500  $\mu$ L Buffer RPE was

pipetted into the column, and again it was centrifuged at 12,000 rpm for 30 seconds. Before adding another 500  $\mu$ L Buffer RPE into the column and centrifuging at 12,000 rpm for 2.5 minutes, the obtained flow and the column were eliminated. The following step included discarding the fluid, replacing the column with a new 2mL collection tube, centrifuging at 12,000 rpm for 2 minutes, and transferring the column to a new 1.5mL collection tube. The final step was pipetting 30  $\mu$ L RNase-free water into the column and waiting five (5) min before centrifuging the RNeasy column at 12,000 rpm for 1.5 minutes. After the final step, the RNA was stored at -80°C for later use or put on ice directly proceeding to quantification, reverse transcription, and RT-PCR [69].

#### Step 2- Quantification of RNA

2  $\mu$ L RNA free water was used as a control to set up the NanoDrop Lite (Fig. 2.6) which is utilized for micro volume measurements of nucleic acid concentration at 260 nm, using the 260/280 ratio and purified protein concentration at 280 nm. The quantifying of RNA was performed by the NanoDrop Lite using 2  $\mu$ L from each sample. The platform was cleaned with a Kimwipe wipers between each sample. The readings were done spectrophotometry and recorded as A260 and A260/280 ratio [69].



Figure 2.6 NanoDrop Lite

The calculation of RNA amount was done as microgram ( $\mu\text{g}$ ) utilizing the following equation;

Equation 3 [69]

$$[RNA] = A_{260} * \left(40 \frac{\mu\text{g}}{\text{mL}}\right) * \text{dilution factor} * \text{RNA volume (mL)} \quad \text{Equation 3 [69]}$$

### Step 3-Generate cDNA with Reverse Transcriptase

The RNA reverse transcription to cDNA was performed by the QuantiTect Reverse Transcription kit in a Bio-Rad S1000 thermal cycler. PCR tubes were labeled according to the number of reactions needed. The QuantiTect Reverse Transcription kit components and RNA samples were put on ice, while a thermocycler was turned on to warm up at 42° C. 200  $\mu\text{L}$  conical tubes were labeled with sample identifiers as one per sample. The volume of RNA sample demanded a 10  $\mu\text{L}$  reaction (generally 10 ng of cDNA will be desired per well for the real-time RT-PCR experiment) were calculated as the following equation which includes 1.10 is for 10% excess [69].

After the RNA volume was calculated, the amount of water required for each reaction was calculated so that the total volume of RNA and the water equaled to 6 $\mu$ L. If the total quantity of total RNA is more than 6  $\mu$ L, there is no requirement for adding water since 6  $\mu$ L of RNA is enough to fulfill the requirement. After calculation, the lack amount of RNA was completed with the demanded amount of water into each 200  $\mu$ L conical tube. Then, one  $\mu$ L of gDNA wipeout was added to each tube, which was mixed with either a pipette or vortex. The required RNA volumes were pipetted into each tube, and the tubes were fused by pipetting and placing into thermocycler to incubate at 42°C for 2 minutes. ‘CAV1’ program was run, and the volume was changed to 10  $\mu$ L. While incubating, 2.5  $\mu$ L of RT buffer/primer mix was combined with 0.5  $\mu$ L reverse transcriptase per sample into a tube. After the incubation was completed, 3  $\mu$ L of reaction buffer mix were put into each PCR tubes and placed back to the incubator for 15 min at 42°C, which was followed by 95°C incubation for 3 minutes. When the incubation time was over, the samples were removed at -20°C [69].

#### Step 4- qPCR – TaqMman

First, the volume of reaction mixture was calculated. The calculation was made as a ten  $\mu$ L reaction volume per well. TaqMan Fast Advanced Master Mix (5  $\mu$ L) constituted the half of the reaction volume. The other half of the amount was composed of 0.5  $\mu$ L TaqMan Gene Expression Assay per well and the mixture of RNase-free water and cDNA. The calculation of the mixture volume of RNase-free water and cDNA per well was made as follows:

$$RVW - MMV - TGEAV = VRfW$$

$$\text{Equation 4 [76]}$$

RVW = Reaction Volume per Well

MMV = Master Mix Volume

TGEAV= TaqMan Gene Expression Assay Volume

VRfW= Volume of RNase-free water and cDNA

Then, the master mix, which consisted of TaqMan Fast Advanced Master Mix and Gene Expression Assay for each gene, was prepared. The total volume of the master mix was calculated in the following way:

$$1.10(x) * NS * NR * (VTMM + VTGEA) = VMM \quad \text{Equation 5 [76]}$$

X = excess solution

NS = Number of samples

NR = Number of replicates/sample

VTMM = Volume of TaqMan Master Mix/reaction

VTGEA = Volume of TaqMan Gene Expression Assay/reaction

VMM = Volume of Master Mix

The cDNA and add RNase-free water solution was thawed, and the total volume of the solution was calculated according to the following equation:

$$1.10 * NS * NR * VRfW = TVRfW \quad \text{Equation 6 [76]}$$

NS= Number of samples

NR= Number of replicates/sample

VRfW= Volume of RNase-free water and cDNA/reaction

TVRfW= Total volume of RNase-free water and cDNA

The master mix was added to the plate and the RNase-free water and cDNA followed it. The plate was sealed with a transparent adhesive before centrifugation. QuantStudio 7 Flex Real-Time PCR System was used to analyze the plate. Results were evaluated utilizing Sequence Detection Systems programming v2.4 (Applied Biosystems) according to the delta-delta Ct strategy. GAPDH was used as the housekeeping gene, and effects were introduced in respect to the GAPDH [76].

Calculations:

Table 2.3. Calculations for TaqMan

<u>TaqMan</u> fast Master Mix=5 $\mu$ Lx[(24x15) +(24x5) +(8x5)] = 2.6 mL
<u>TaqMan</u> gene expression assay= 0.5 $\mu$ L/well
Master mix 2 (sample)= 10 $\mu$ L- <u>TaqMan</u> master mix (5 $\mu$ L)- <u>TaqMan</u> gene expression (0.5 $\mu$ L) = 4.5 $\mu$ L
Master Mix 2 (gene mix) = 1.1x130x (5 $\mu$ L+ 0.5 $\mu$ L) (715 $\mu$ L fast + 71.5 $\mu$ L primer)
Master mix2 (cDNA)= 4.5 $\mu$ Lx1.1x8= 39.6 total volume (10 $\mu$ L cDNA and 29.6 $\mu$ L water for each sample



## 2.6. Statistical analysis

One-way analysis of variance (ANOVA) was performed on metabolic activity and gene expressions. Significance was set at  $p < 0.05$ . Analysis of metabolic activity included  $n = 3$  samples per group while gene expressions used  $n = 5$  samples per group. The standard errors of the means were reported in the figures. There were significant differences between groups and days.

## 2.7. Results and Discussion

A synthetic bone substitute requires a porous matrix, which has an interconnecting porosity that increases rapid bone growth. Also, it should have adequate strength to preserve its mechanical properties under physical loads. It should also form a secure framework that allows and stimulates growth and penetration of new cells into pores. One possibility to meet these requirements is to utilize porous materials that allow new bone and tissue formation by permitting the cells growth into pores because the large surface area of pores permits cell attachment, growth, and differentiation [77]. Biomaterials with mineral content have a significant role in tissue engineering; they are accepted as osteoconductive biomaterials and generate a potential biological bone substitute [78]. The need of porous materials which not only allow new bone formation but also are able to blend with mineral is crucial for bone substitute materials. Therefore, neat and composite (10HA%+ATSP oligomers) porous samples of ATSP were fabricated. Both neat and composite foam samples were seeded with MSCs and cultured for one, four, and seven days. The foam samples were cultured in growth and osteogenic media. The groups were categorized as: (i) scaffold(neat samples) with growth media (SGM), (ii) composite with growth media (CGM), (iii) scaffold with osteogenic media (SOM), and (iv) composite with osteogenic media (COM). During the culture period, the mitochondrial metabolic activity of

MSCs on the samples was measured by using an alamarBlue® absorbance assay. Samples were seeded with MSC and incubated in alamarBlue® solution for 2.5 hours. AlamarBlue® dye was reduced by viable cells to a fluorescent byproduct (resorufin). Absorbance values were used to calculate the reduction of alamarBlue® (excitation: 570 nm, emission: 600 nm). The reduction of alamarBlue® was calculated according to the equation provided by the manufacturer (Table 13) and the experiments were performed in triplicate [79].

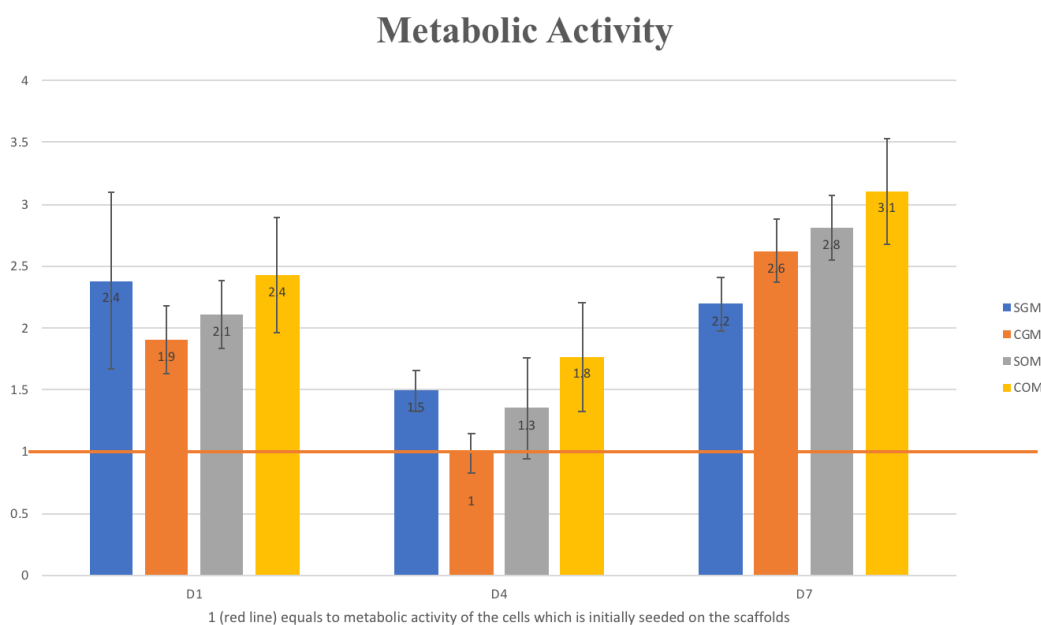


Figure 2.7 The metabolic activity of foam samples with alamar blue by MSCs

MSC metabolic activity was performed by alamarBlue® (Figure 2.7). Through the experiment, the results were compared to the red line which corresponds to 1 (threshold). This value (1) was accepted as the metabolic cell activity of the cells which were initially seeded on the samples. The highest metabolic activities were found in SGM and COM in day one, and none of the samples showed a toxic effect; the results for all samples were higher than initial metabolic activity values (greater than one). The samples did not cause cell death and allowed the cell proliferation. Statistical analysis also showed a significant effect of both the culture time

and scaffold type ( $p < 0.05$ ). All of the results on day four were less than the results of the first day. However, they were still higher than or at least equal to the threshold value (greater than or equal to one). For day seven, the pattern belonged to CGM, SOM, and COM were analogous to other days' patterns; however, the result for SGM was different. CGM, SOM, and COM were initially behind the SGM, but they eventually approached and even surpassed the metabolic activity of the SGM at day seven ( $p < 0.05$ ). The results showed that mineralized samples had a positive effect on the metabolic activity because the composite samples showed high metabolic activity in comparison to neat samples on day seven ( $p < 0.05$ ). Also, osteogenic groups (SOM and COM) demonstrated the highest metabolic activity compared to the other groups on day seven. The metabolic activity of all the samples on day seven was significantly higher than the threshold level ( $p < 0.05$ ). Therefore, it could be said that our samples were allowing cell proliferating and growth. Moreover, since all of the results were above the standard line, our samples did not cause cell death.

The expression levels osteogenic encrypting for osteopontin (SPP1), bone sialoprotein 2 (IBSP), and runt-related translation factor 2 (RUNX2) were measured after one, four, and seven days in growth and osteogenic media culture (Figure 2.8). All the data were analyzed by comparison between the initial expression value shown in the graph with a red line for each figure and the results obtained on the day seven. Also, if the results were higher than the initial value at day seven, it was defined as upregulated, which means it was increasing the gene expressing. On the other hand, if the result was less than the initial value, it was described as a downregulated.

These results showed that there was a complex trend in a response to scaffold type (neat versus scaffold) and media type ( $p < 0.05$ ). The samples in the osteogenic induction media had a

greater effect on osteogenic gene expression than the material type. Statistical analysis demonstrated a significant effect of both the culture media and scaffold type ( $p < 0.05$ ).

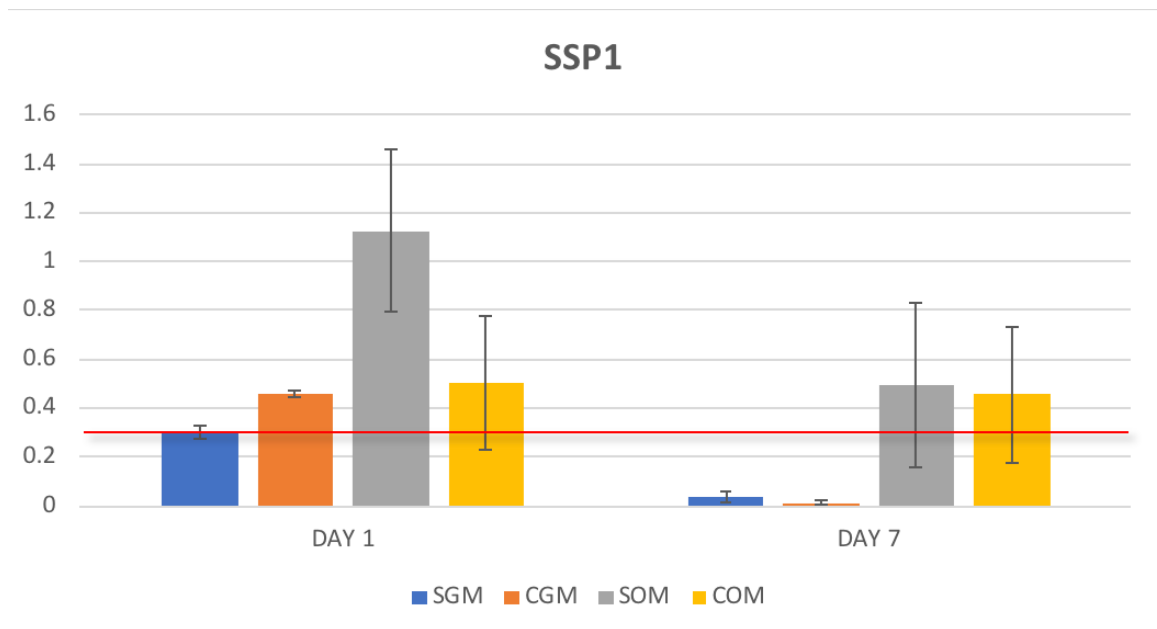


Figure 2.8 The results of SSP1 expression

Regardless of the medium type, the day one SPP1 expression for all of the samples was either higher than or equal to the initial gene expression value. However, the expression of SPP1 for the samples in growth media was downregulated; the expression levels decreased slightly on day seven. The osteogenic groups (Figure 2.8) demonstrated the highest level of osteogenesis on day seven ( $p < 0.05$ ). While SOM showed a slight decrease, COM groups did not demonstrate a decrease, and there were no significant differences between SOM and COM groups on day seven ( $p < 0.05$ ). Neat and composite samples in the combination with osteogenic media had higher levels SPP1 expression than mineralized one ( $p < 0.05$ ). The presence of the SSP1 expression in

the results suggests that this material can act as a structural substance since this gene regulates the biomineralization.

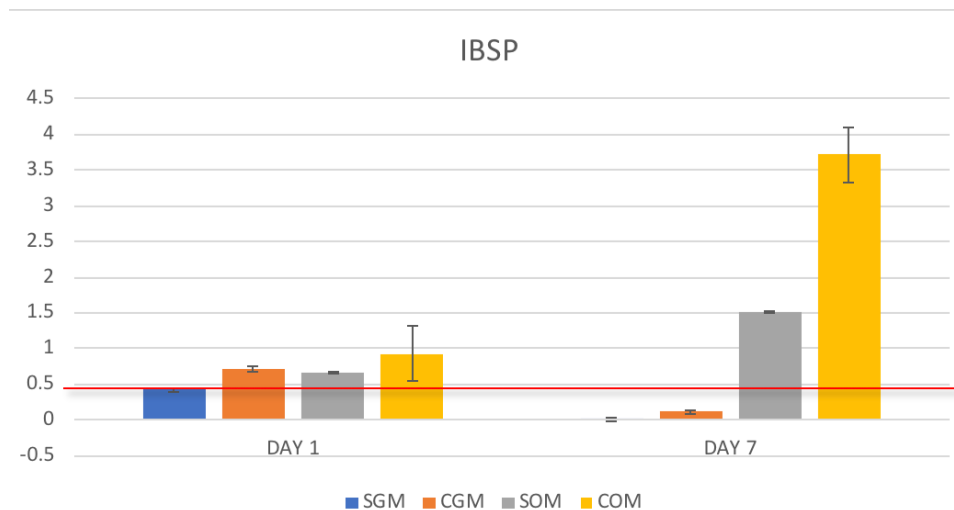


Figure 2.9 The results of IBSP expression

However, the trend in the SPP1 expression for samples in growth media was similar to the IBSP expression; the composite and neat samples in growth media did not promote the osteogenic responses. However, the IBSP expression level for neat and mineralized group in osteogenic media was up-regulated from day one to day seven and was higher than the other groups at day seven ( $p < 0.05$ ) (Fig 2.9). The expressions of IBSP are mostly observed in mineralized tissue and advances mineral formation in the bone. The high-level expression of IBSP results in the mineral and nodule formation and increase in the osteoblast related gene expression. Therefore, our samples in the osteogenic media allowed mineral formation.

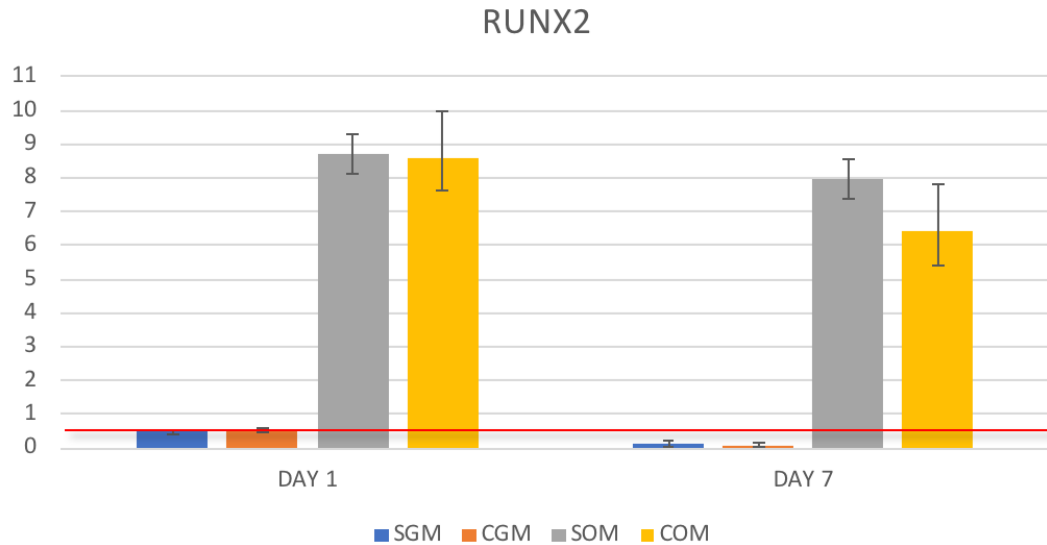


Figure 2.10 The results of RUNX2 expression

Like the others, the RUNX2 expression of neat and composite samples in the growth media showed the similar pattern, they were downregulated. Osteogenic groups were upregulated ( $p < 0.05$ ) and there was no significant decrease in osteogenic groups for RUNX2 expression. The mineralized and neat samples in growth media did not drive the osteogenic response while neat and composite samples in osteogenic media showed high osteogenic response. Increase in the expression of Runx-2 results in sufficient bone formation since RUNX2 gene is viewed as a main controller of osteogenesis. For all the results, the samples in osteogenic media showed upregulated pattern for all gene expressions. Hence, samples in osteogenic media allows new bone formation. It can also be said that neat and mineralized samples in combination with pure osteogenic medium promote optimal osteogenesis ( $p < 0.05$ ) (Fig. 2.10)

## 2.8. Future Works

Although the studies were promising, more long term investigations must be done. Additional factor combinations or different dosage can be applied to explore their effects in future studies. Combining the growth factors with biomaterial is still being developed in other studies; this approach could be critical and important for repairing complex orthopedic injuries.

## REFERENCES

- [1] Huang, Y., & Economy, J. (2007). Aromatic Thermosetting Copolyester (ATSP)/UHMWPE Blends with improved wear properties and biocompatibility. *MRS Proceedings*, 1063  
doi:10.1557/proc-1063-oo09-09
- [2] Synthetic materials in medicine. (n.d.). *Chemistry of Medical and Dental Materials*, 1-24.  
doi:10.1039/9781847552051-00001
- [3] Ramakrishna, S., Mayer, J., Wintermantel, E., & Leong, K. W. (2001). Biomedical applications of polymer-composite materials: A review. *Composites Science and Technology*, 61(9), 1189-1224. doi:10.1016/s0266-3538(00)00241-4
- [4] Deluca, P. A., Lindsey, R. W., & Ruwe, P. A. (1988). Refracture of bones of the forearm after the removal of compression plates. *The Journal of Bone & Joint Surgery*, 70(9), 1372-1376.  
doi:10.2106/00004623-198870090-00015
- [5] Maitz, M. (2015). Applications of synthetic polymers in clinical medicine. *Biosurface and Biotribology*, 1(3), 161-176. doi: 10.1016/j.bsbt.2015.08.002
- [6] Burny, F., Donkerwolcke, M., & Muster, D. (1995). Biomaterials education: A challenge for medicine and industry in the late 1990s. *Materials Science and Engineering: A*, 199(1), 53-59.  
doi:10.1016/0921-5093(95)09907-7
- [7] Williams, D. F., & European Society for Biomaterials. (1987). *Definitions in biomaterials: Proceedings of a consensus conference of the European Society for Biomaterials, Chester, England, March 3-5, 1986*. Amsterdam: Elsevier.
- [8] Anderson, J. M. (1983). Biological performance of materials-fundamentals of biocompatibility *Journal of Biomedical Materials Research*, 17(3), 557-558.  
doi:10.1002/jbm.820170313.
- [9] Orlovskii, V. P., et al. "Inorganic Materials." *Inorganic Materials*, vol. 38, no. 10, 2002, pp. 973–984., doi:10.1023/a:1020585800572.
- [10] Anderson, J. M. (2001). Biological responses to materials. *Annual Review of Materials Research*, 31(1), 81-110. doi: 10.1146/annurev.matsci.31.1.81
- [11] Amato, S. (2015). Regulatory strategies for biomaterials and medical devices in the USA: Classification, design, and risk analysis. *Regulatory Affairs for Biomaterials and Medical Devices*, 27-46. doi:10.1533/9780857099204.27
- [12] Dorozhkin, Sergey V. "Calcium orthophosphate-based bioceramics and biocomposites." Feb. 2016, doi:10.1002/9783527699315.



- [13] Williams, D. F. Tissue-biomaterial interactions. *Journal of Materials Science*, vol. 22, no. 10, 1987, pp. 3421–3445., doi:10.1007/bf01161439.
- [14] Isa, Z.M., and J.M. Hobkirk. Dental implants: Biomaterial, biomechanical and biological considerations.” *Annals of Dentistry*, vol. 7, no. 1, 2000, pp. 27–35., doi: 10.22452/adum.vol7no1.6.
- [15] Crubézy, Eric, et al. “Identification of mycobacterium DNA in an Egyptian Potts Disease of 5400 years old.” *Comptes Rendus De L'Académie Des Sciences - Series III - Sciences De La Vie*, vol. 321, no. 11, 1998, pp. 941–951., doi:10.1016/s0764-4469(99)80009-2.
- [16] Kara, Sadik. *A Roadmap of Biomedical Engineers and Milestones*. InTech, 2012.
- [17] Niinomi, Mitsuo. Recent research and development in metallic materials for biomedical, dental and healthcare products applications. *Materials Science Forum*, vol. 539-543, 2007, pp. 193–200., doi: 10.4028/www.scientific.net/msf.539-543.193.
- [18] Silver, Frederick H. *Biomaterials Science and Biocompatibility*. Springer, 1999.
- [19] Frich, D., Goranov, K., Schneggenburger, L., & Economy, J. (1996). Novel High-Temperature Aromatic Copolyester Thermosets: Synthesis, Characterization, and Physical Properties. *Macromolecules*, 29(24), 7734-7739. doi:10.1021/ma960862d
- [20] Vaezian, B., Meyer, J. L., & Economy, J. (2016). Processing of aromatic thermosetting copolyesters into foams and bulk parts: Characterization and mechanical properties. *Polymers for Advanced Technologies*, 27(8), 1006-1013. doi:10.1002/pat.3762
- [21] Parkar, Z., Economy, J., Economy, J., Geil, P. H., Sottos, N., & Cheng, J. (2011). *Design of unique composites based on aromatic thermosetting copolyesters* (Unpublished master's thesis).
- [22] Rattier, B. D., Hoffman, A. S., Schoen, F. J., & Lemons, J. E. (1997). Biomaterials science. *Journal of Clinical Engineering*, 22(1), 26. doi:10.1097/00004669-199701000-00009
- [23] Nanotechnology Applications for Tissue Engineering. (2015). doi:10.1016/c2014-0-00006-8
- [24] Boutrand, J. (2017). *Biocompatibility and Performance of Medical Devices*. S.L.: Woodhead.
- [25] Ratner, B. D. (2015). The Biocompatibility of Implant Materials. *Host Response to Biomaterials*, 37-51. doi:10.1016/b978-0-12-800196-7.00003-7
- [26] Cosmetic Dentistry in Ancient Time – Short Review. (n.d.). Retrieved from [https://www.bing.com/cr?IG=04598C4784404EB28A2E2EE449535154&CID=19519472F8196B0E112F9856F9E46AA1&rd=1&h=tV9eR97wDCEmIDkGzgcIFpxMtFZJtoZhaR\\_6jDEYmE8&v=1&r=https://www.researchgate.net/publication/230777774\\_Cosmetic\\_Dentistry\\_in\\_Ancient\\_Time\\_-\\_Short\\_Review&p=DevEx.LB.1,5566.1](https://www.bing.com/cr?IG=04598C4784404EB28A2E2EE449535154&CID=19519472F8196B0E112F9856F9E46AA1&rd=1&h=tV9eR97wDCEmIDkGzgcIFpxMtFZJtoZhaR_6jDEYmE8&v=1&r=https://www.researchgate.net/publication/230777774_Cosmetic_Dentistry_in_Ancient_Time_-_Short_Review&p=DevEx.LB.1,5566.1)

- [27] Crubzy, E., Murail, P., Girard, L., & Bernadou, J. (1998). False teeth of the Roman world. *Nature*, 391(6662), 29-29. doi:10.1038/34067
- [28] Apple, D. J., & Sims, J. (1996). Harold Ridley and the invention of the intraocular lens. *Survey of Ophthalmology*, 40(4), 279-292. doi:10.1016/s0039-6257(96)82003-0
- [29] Homsy, C. A. (1970). Bio-Compatibility in selection of materials for implantation. *Journal of Biomedical Materials Research*, 4(3), 341-356. doi:10.1002/jbm.820040306
- [29] Homsy, C. A., Ansevin, K. D., Obannon, W., Thompson, S. A., Hodge, R., & Estrella, M. E. (1970). Rapid In-vitro Screening of Polymers for Biocompatibility. *Journal of Macromolecular Science: Part A - Chemistry*, 4(3), 615-634. doi:10.1080/00222337008074366
- [31] Isabel Cristina Celerino De Moraes Porto. (2012). Polymer Biocompatibility. *Polymerization*. doi:10.5772/47786
- [32] International Organization for Standardization (ISO). (n.d.). *SpringerReference*. doi:10.1007/springerreference\_76157
- [33] ISO - International Organization for Standardization. (2017, February 09). Retrieved from <https://www.iso.org/standard/36406.html>
- [34] ISO - International Organization for Standardization. (2002, September 26). Retrieved from <https://www.iso.org/standard/18971.html>
- [35] ISO - International Organization for Standardization. (2017, September 14). Retrieved from <https://www.iso.org/standard/35977.html>
- [36] ISO - International Organization for Standardization. (2014, September 24). Retrieved from <https://www.iso.org/standard/55614.html>
- [37] ISO - International Organization for Standardization. (2016, November 28). Retrieved from <https://www.iso.org/standard/61089.html>
- [38] ISO - International Organization for Standardization. (2017, April 12). Retrieved from <https://www.iso.org/standard/63448.html>
- [39] ISO - International Organization for Standardization. (2013, July 09). Retrieved from <https://www.iso.org/standard/44049.html>
- [40] ISO - International Organization for Standardization. (2014, October 10). Retrieved from <https://www.iso.org/standard/44908.html>
- [41] Jong, W. D., Carraway, J., & Geertsma, R. (2012). In-vivo and in-vitro testing for the biological safety evaluation of biomaterials and medical devices. *Biocompatibility and Performance of Medical Devices*, 120-158. doi:10.1533/9780857096456.2.120.

- [42] Li, W., Zhou, J., & Xu, Y. (2015). Study of the in-vitro cytotoxicity testing of medical devices. *Biomedical Reports*, 3(5), 617-620. doi:10.3892/br.2015.481
- [43] Ratner, B. D., Hoffman, A. S., Schoen, F. J., & Lemons, J. E. (2014). *Biomaterials Science: An Introduction to Materials in Medicine*. Saint Louis: Elsevier Science.
- [44] Apoptosis, Cytotoxicity and Cell Proliferation. (n.d.). Retrieved from [https://www.google.com/url?sa=t&rct=j&q=&esrc=s&source=web&cd=2&cad=rja&uact=8&ved=0ahUKEwjkk7h6qvcAhXHxYMKHXfmB3cQFgg0MAE&url=https://www.researchgate.net/profile/Massakib\\_Bekkaye2/post/Dose\\_anyone\\_know\\_about\\_programmed\\_cell\\_death\\_in\\_plants/attachment/59d62fecc49f478072ea03d1/AS:273594888720388@1442241514779/download/05242134001\\_05.08.pdf&usg=AOvVaw00XW4YTDp0daIHLz2kX6WM](https://www.google.com/url?sa=t&rct=j&q=&esrc=s&source=web&cd=2&cad=rja&uact=8&ved=0ahUKEwjkk7h6qvcAhXHxYMKHXfmB3cQFgg0MAE&url=https://www.researchgate.net/profile/Massakib_Bekkaye2/post/Dose_anyone_know_about_programmed_cell_death_in_plants/attachment/59d62fecc49f478072ea03d1/AS:273594888720388@1442241514779/download/05242134001_05.08.pdf&usg=AOvVaw00XW4YTDp0daIHLz2kX6WM)
- [45] Elliott, W. M., & Auersperg, N. (1993). Comparison of the Neutral Red and Methylene Blue Assays to study cell growth in culture. *Biotechnic & Histochemistry*, 68(1), 29-35. doi:10.3109/10520299309105573
- [46] Decker, T., & Lohmann-Matthes, M. (1988). A quick and simple method for the quantitation of lactate dehydrogenase release in measurements of cellular cytotoxicity and tumor necrosis factor (TNF) activity. *Journal of Immunological Methods*, 115(1), 61-69. doi:10.1016/0022-1759(88)90310-9
- [47] Jabbar, S., Twentyman, P., & Watson, J. (1989). The MTT assay underestimates the growth inhibitory effects of interferons. *British Journal of Cancer*, 60(4), 523-528. doi:10.1038/bjc.1989.306
- [48] Carmichael, J., Mitchell, J., Degraff, W., Gamson, J., Gazdar, A., Johnson, B., . . . Minna, J. (1988). Chemosensitivity testing of human lung cancer cell lines using the MTT assay. *British Journal of Cancer*, 57(6), 540-547. doi:10.1038/bjc.1988.125
- [49] A Review on Di Methyl Thiazoldiphenyl-Tetrazoliumbromide (MTT) Assay in Cell Viability. (n.d.). Retrieved from <https://www.medwelljournals.com/abstract/?doi=rjasci.2017.372.378>
- [50] Berridge, M. V., Herst, P. M., & Tan, A. S. (2005). Tetrazolium dyes as tools in cell biology: New insights into their cellular reduction. *Biotechnology Annual Review*, 127-152. doi:10.1016/s1387-2656(05)11004-7
- [51] Page, B., Page, M., & Noel, C. (1993). A new fluorometric assay for cytotoxicity measurements in-vitro. *International Journal of Oncology*. doi:10.3892/ijo.3.3.473
- [52] O'Brien, J., Wilson, I., Orton, T., & Pognan, F. (2000). Investigation of the Alamar Blue (resazurin) fluorescent dye for the assessment of mammalian cell cytotoxicity. *European Journal of Biochemistry*, 267(17), 5421-5426. doi:10.1046/j.1432-1327.2000.01606.x

- [53] Ahmed, S. A., Gogal, R. M., & Walsh, J. E. (1994). A new rapid and simple non-radioactive assay to monitor and determine the proliferation of lymphocytes: An alternative to [<sup>3</sup>H] thymidine incorporation assay. *Journal of Immunological Methods*, 170(2), 211-224. doi:10.1016/0022-1759(94)90396-4
- [54] U.S. Patent No. 5,501,959. (1996). Washington, DC: U.S. Patent and Trademark Office. The alamarBlue® Assay
- [55] Tonder, A. V., Joubert, A. M., & Cromarty, A. (2015). Limitations of the 3-(4,5-dimethylthiazol-2-yl)-2,5-diphenyl-2H-tetrazolium bromide (MTT) assay when compared to three commonly used cell enumeration assays. *BMC Research Notes*, 8(1), 47. doi:10.1186/s13104-015-1000-8
- [56] Dai, Z., Ronholm, J., Tian, Y., Sethi, B., & Cao, X. (2016). Sterilization techniques for biodegradable scaffolds in tissue engineering applications. *Journal of Tissue Engineering*, 7, 204173141664881. doi:10.1177/2041731416648810
- [57] Schindelin, J., Arganda-Carreras, I., Frise, E., Kaynig, V., Longair, M., Pietzsch, T., . . . Cardona, A. (2012). Fiji: An open-source platform for biological-image analysis. *Nature Methods*, 9(7), 676-682. doi:10.1038/nmeth.2019
- [58] Kumar, P., Nagarajan, A., & Uchil, P. D. (2018). Analysis of cell viability by the MTT Assay. *Cold Spring Harbor Protocols*, 2018(6). doi:10.1101/pdb.prot095505
- [59] Cenni, E., Ciapetti, G., Granchi, D., Arciola, C., Savarino, L., Stea, S., . . . Pizzoferrato, A. (1999). Established cell lines and primary cultures in testing medical devices in-vitro. *Toxicology in-vitro*, 13(4-5), 801-810. doi:10.1016/s0887-2333(99)00058-2
- [60] Riss, T. L. (2016, July 01). Cell viability assays. Retrieved from <https://www.ncbi.nlm.nih.gov/books/NBK144065/>
- [61] Bongio, M., Van Den Beucken, J.J.J.P., Leeuwenburgh, S.C.G., Jansen, J.A. (2010). Development of bone substitute materials: From 'biocompatible' to 'instructive'. *Journal of Materials Chemistry*, 20 (40), pp. 8747-8759
- [62] Roeder, R. K., Converse, G. L., Kane, R. J., & Yue, W. (2008). Hydroxyapatite-reinforced polymer biocomposites for synthetic bone substitutes. *Jom*, 60(3), 38-45. doi:10.1007/s11837-008-0030-2
- [63] Ullah, I., Subbarao, R., & Rho, G. (2015). Human mesenchymal stem cells - current trends and future prospective. *Bioscience Reports*, 35(2), 1-18. doi:10.1042/bsr20150025
- [64] Engler, A. J., Sen, S., Sweeney, H. L., & Discher, D. E. (2006). Matrix elasticity directs stem cell lineage specification. *Cell*, 126(4), 677-689. doi: 10.1016/j.cell.2006.06.044

- [65] Lin, X., Shi, Y., Cao, Y., & Liu, W. (2016). Recent progress in stem cell differentiation directed by material and mechanical cues. *Biomedical Materials*, 11(1), 014109. doi:10.1088/1748-6041/11/1/014109
- [66] Dantò, V., Raucci, M. G., Guarino, V., Martina, S., Valletta, R., & Ambrosio, L. (2013). Behaviour of human mesenchymal stem cells on chemically synthesized HA-PCL scaffolds for hard tissue regeneration. *Journal of Tissue Engineering and Regenerative Medicine*, 10(2). doi:10.1002/term.1768
- [67] Michel, J., Penna, M., Kochen, J., & Cheung, H. (2015). Recent advances in hydroxyapatite scaffolds containing mesenchymal stem cells. *Stem Cells International*, 2015, 1-13. doi:10.1155/2015/305217
- [68] Rogina, A., Antunović, M., Pribolšan, L., Mihalić, K. C., Vukasović, A., Ivković, A., . . . Ivanković, H. (2017). Human mesenchymal stem cells differentiation regulated by hydroxyapatite content within chitosan-based scaffolds under perfusion conditions. *Polymers*, 9(12), 387. doi:10.3390/polym9090387
- [69] Caliarì, S. R., Harley, B. A., Higdon, J. J., Bailey, R. C., Rao, C. V., & Kong, H. J. (n.d.). *The influence of collagen-GAG scaffold architectural and biological cues on tenocyte and mesenchymal stem cell bioactivity for musculoskeletal tissue engineering* (Unpublished master's thesis).
- [ 70] Mendes, G. C., Brandão, T. R., & Silva, C. L. (2007). Ethylene oxide sterilization of medical devices: A review. *American Journal of Infection Control*, 35(9), 574-581. doi: 10.1016/j.ajic.2006.10.014
- [71] Fraga, D., Meulia, T., & Fenster, S. (2008). Real-time PCR. *Current protocols essential laboratory techniques*, (1), 10-3.
- [72] Biosystems, A. (2004). Guide to performing relative quantitation of gene expression using real-time quantitative PCR. *Applied Biosystems*
- [73] Gordon, J. A., Tye, C. E., Sampaio, A. V., Underhill, T. M., Hunter, G. K., & Goldberg, H. A. (2007). Bone sialoprotein expression enhances osteoblast differentiation and matrix mineralization in-vitro. *Bone*, 41(3), 462-473. doi: 10.1016/j.bone.2007.04.191
- [74] Granéli, C., Thorfve, A., Ruetschi, U., Brisby, H., Thomsen, P., Lindahl, A., & Karlsson, C. (2014). Novel markers of osteogenic and adipogenic differentiation of human bone marrow stromal cells identified using a quantitative proteomics approach. *Stem Cell Research*, 12(1), 153-165. doi: 10.1016/j.scr.2013.09.009
- [75] Mcfadden, T., Duffy, G., Allen, A., Stevens, H., Schwarzmaier, S., Plesnila, N., . . . O'Brien, F. (2013). The delayed addition of human mesenchymal stem cells to pre-formed endothelial cell networks results in functional vascularization of a collagen–glycosaminoglycan scaffold in vivo. *Acta Biomaterialia*, 9(12), 9303-9316. doi: 10.1016/j.actbio.2013.08.014

[76] TaqMan® Gene Expression Assays Protocol. (n.d.). Retrieved from <http://www5.appliedbiosystems.com/mutation-detection/>

[77] Deville, S., Saiz, E., & Tomsia, A. P. (2006). Freeze casting of hydroxyapatite scaffolds for bone tissue engineering. *Biomaterials*, 27(32), 5480-5489. doi: 10.1016/j.biomaterials.2006.06.028

[78] Westhrin, M., Xie, M., Olderøy, M. Ø, Sikorski, P., Strand, B. L., & Standal, T. (2015). Osteogenic Differentiation of Human Mesenchymal Stem Cells in Mineralized Alginate Matrices. *Plos One*, 10(3). doi: 10.1371/journal.pone.0120374

[79] AlamarBlue® - Bio-Rad Antibodies. (n.d.). Retrieved from <https://www.bio-rad-antibodies.com/static/uploads/ifu/buf012a.pdf>